AGU PUBLICATIONS

Tectonics

RESEARCH ARTICLE
10.1002/2016TC004206

Kinematics of a former oceanic plate of the Neotethys revealed by deformation in the Ulukışla basin (Turkey)

Derya Gürer[1], Douwe J. J. van Hinsbergen[1], Liviu Matenco[1], Fernando Corfu[2,3], and Antonio Cascella[4]

[1]Department of Earth Sciences, University of Utrecht, Utrecht, Netherlands, [2]Department of Geosciences, University of Oslo, Oslo, Norway, [3]Centre for Earth Evolution and Dynamics, University of Oslo, Oslo, Norway, [4]Istituto Nazionale di Geofisica e Vulcanologia, Pisa, Italy

Key Points:
- Cretaceous to Paleocene N-S and E-W extension was overprinted by Eo-Oligocene shortening
- The geology of Central Anatolia can be explained by a three-plate system in Cretaceous to Paleogene time
- We reconstruct upper plate kinematics to infer subduction evolution and relative plate and trench motions within the Neotethyan ocean

Supporting Information:
- Supporting Information S1

Correspondence to:
D. Gürer,
m.d.gurer@uu.nl

Citation:
Gürer, D., D. J. J. van Hinsbergen, L. Matenco, F. Corfu, and A. Cascella (2016), Kinematics of a former oceanic plate of the Neotethys revealed by deformation in the Ulukışla basin (Turkey), *Tectonics*, *35*, 2385–2416, doi:10.1002/2016TC004206.

Received 11 APR 2016
Accepted 30 AUG 2016
Accepted article online 9 SEP 2016
Published online 19 OCT 2016

Abstract Kinematic reconstruction of modern ocean basins shows that since Pangea breakup a vast area in the Neotethyan realm was lost to subduction. Here we develop a first-order methodology to reconstruct the kinematic history of the lost plates of the Neotethys, using records of subducted plates accreted to (former) overriding plates, combined with the kinematic analysis of overriding plate extension and shortening. In Cretaceous-Paleogene times, most of Anatolia formed a separate tectonic plate—here termed "Anadolu Plate"—that floored part of the Neotethyan oceanic realm, separated from Eurasia and Africa by subduction zones. We study the sedimentary and structural history of the Ulukışla basin (Turkey); overlying relics of this plate to reconstruct the tectonic history of the oceanic plate and its surrounding trenches, relative to Africa and Eurasia. Our results show that Upper Cretaceous-Oligocene sediments were deposited on the newly dated suprasubduction zone ophiolites (~92 Ma), which are underlain by mélanges, metamorphosed and nonmetamorphosed oceanic and continental rocks derived from the African Plate. The Ulukışla basin underwent latest Cretaceous-Paleocene N-S and E-W extension until ~56 Ma. Following a short period of tectonic quiescence, Eo-Oligocene N-S contraction formed the folded structure of the Bolkar Mountains, as well as subordinate contractional structures within the basin. We conceptually explain the transition from extension, to quiescence, to shortening as slowdown of the Anadolu Plate relative to the northward advancing Africa-Anadolu trench resulting from collision of continental rocks accreted to Anadolu with Eurasia, until the gradual demise of the Anadolu-Eurasia subduction zone.

1. Introduction

The simultaneous activity of two parallel subduction plate boundaries in line and dipping in the same direction leads to complex geodynamics and slab-mantle interactions. This also results in a complex interplay between trench retreat and advance [*Funiciello et al*., 2008; *Schellart et al*., 2008; *Čížková and Bina*, 2015; *Williams et al*., 2015]. A recent numerical modeling study suggests that two parallel subduction zones in line may lead to extreme plate motion and trench advance rates [*Jagoutz et al*., 2015]. Natural examples of such systems, however, are rare and remain poorly studied.

From the geological record that remains of the paleogeographic domain covered by the Neotethys ocean, which separated Gondwana-derived continents from Eurasia, multiple synchronous subduction zones have been interpreted for Cretaceous to Paleogene time [e.g., *Dewey and Şengör*, 1979; *Şengör and Yılmaz*, 1981; *Dixon and Robertson*, 1984; *Okay*, 1986; *Robertson et al*., 2009; *Lefebvre et al*., 2013; *Jagoutz et al*., 2015; *Menant et al*., 2016]. These subduction zones were generally northward dipping and should have surrounded oceanic lithospheric plates in a fashion reminiscent of today's Philippine Sea [*Seno and Maruyama*, 1984; *Hall*, 2002; *Gaina and Müller*, 2007; *Zahirovic et al*., 2014; *Wu et al*., 2016], i.e., oceanic lithosphere forming the overriding plate to one subduction system and the downgoing plate to another [e.g., *van Hinsbergen et al*., 2016]. Such complex evolution involved the interaction of several microplates, oceanic basins, and intervening magmatic arcs.

A well-known terminology issue in Mediterranean studies is the definition of fore-arc and back-arc domains and associated sedimentary basins that relies otherwise on the position of magmatic arcs created during subduction [e.g., *Uyeda and Kanamori*, 1979; *Dewey*, 1980]. The rapid retreat of Mediterranean slabs, often composed of delaminated mantle lithosphere, has resulted in situations where such magmatic arcs are absent, strongly dismembered, often with no direct link with coeval subduction or surpassed by the retreat from a fore-arc to a back-arc position [e.g., *Jolivet and Brun*, 2010; *Carminati et al*., 2012; *Faccenna et al*., 2014].

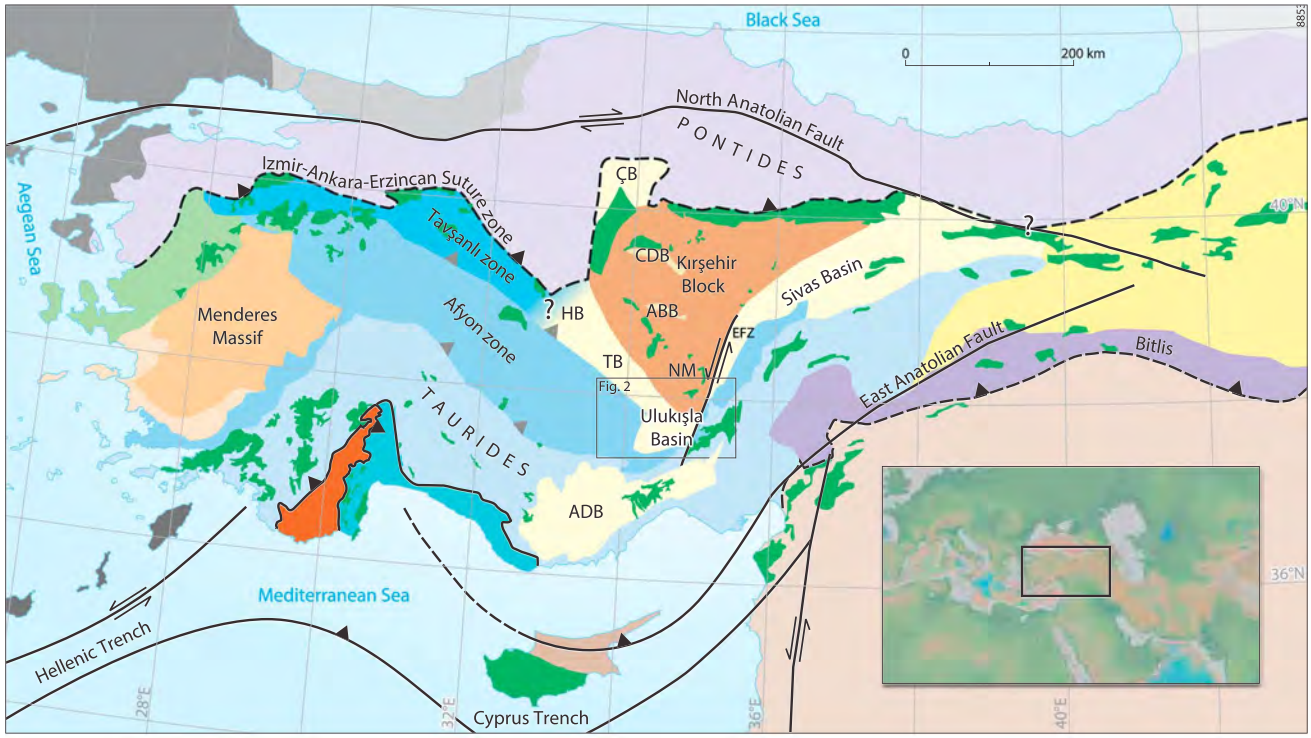

Figure 1. Map of Late Cretaceous to Miocene sedimentary basins of Central Anatolia in the framework of the tectono-metamorphic units of the Eastern Mediterranean, associated suture zones, ophiolites, and major faults (modified after *Okay et al*. [1996], *Pourteau et al*. [2010], and *van Hinsbergen and Schmid* [2012]). The basement units are the Pontides, the HT-metamorphic Kırşehir block (with its southern tip the Niğde Massif (NM)), the Tavşanlı, and Afyon metamorphic HP-belts. Central Anatolian basins mentioned in the text: Ulukışla basin (this study; Figure 2), ÇB = Çankırı basin, ÇDB = Çiçekdağı basin, ABB = Ayhan-Büyükkışla basin, HB = Haymana basin, TB = Tuzgölü basin, ADB = Adana basin, Sivas basin. Major faults marked include the North Anatolian fault and the Ecemiş Fault zone (EFZ), East Anatolian Fault.

Therefore, similar with other fore-arc and back-arc studies [*Fuller et al*., 2006; *Jolivet et al*., 2013], we use the term fore-arc basin as the sedimentation area overlying the transitional contact between the frontal part of the overriding plate, its active deforming thrusting wedge, and the downgoing plate during the coeval oceanic or continental subduction.

Such fore-arc and back-arc processes are relevant in the geological record of Central Anatolia (Figure 1), interpreted to result from the interplay between a southern subduction zone, which started within oceanic lithosphere in Late Cretaceous time (~100–95 Ma) [*Dilek et al*., 1999; *Robertson et al*., 2012; *van Hinsbergen et al*., 2016] and is still active today, and a northern one that was been active from at least ~130 Ma [e.g., *Okay et al*., 2006] until it terminated in the Paleogene [*Keskin*, 2007; *Kaymakci et al*., 2009; *Meijers et al*., 2010; *Espurt et al*., 2014]. Paleogeographically, the Pontides and the Taurides were separated by a domain floored by oceanic crust. This is the Neotethyan oceanic plate system, which must have existed across an area reaching as far east as India ("NOP", after *van Hinsbergen et al*. [2016]. This plate system comprised oceanic lithosphere that underlay part of the Neotethys oceanic realm and was surrounded by subduction zones.

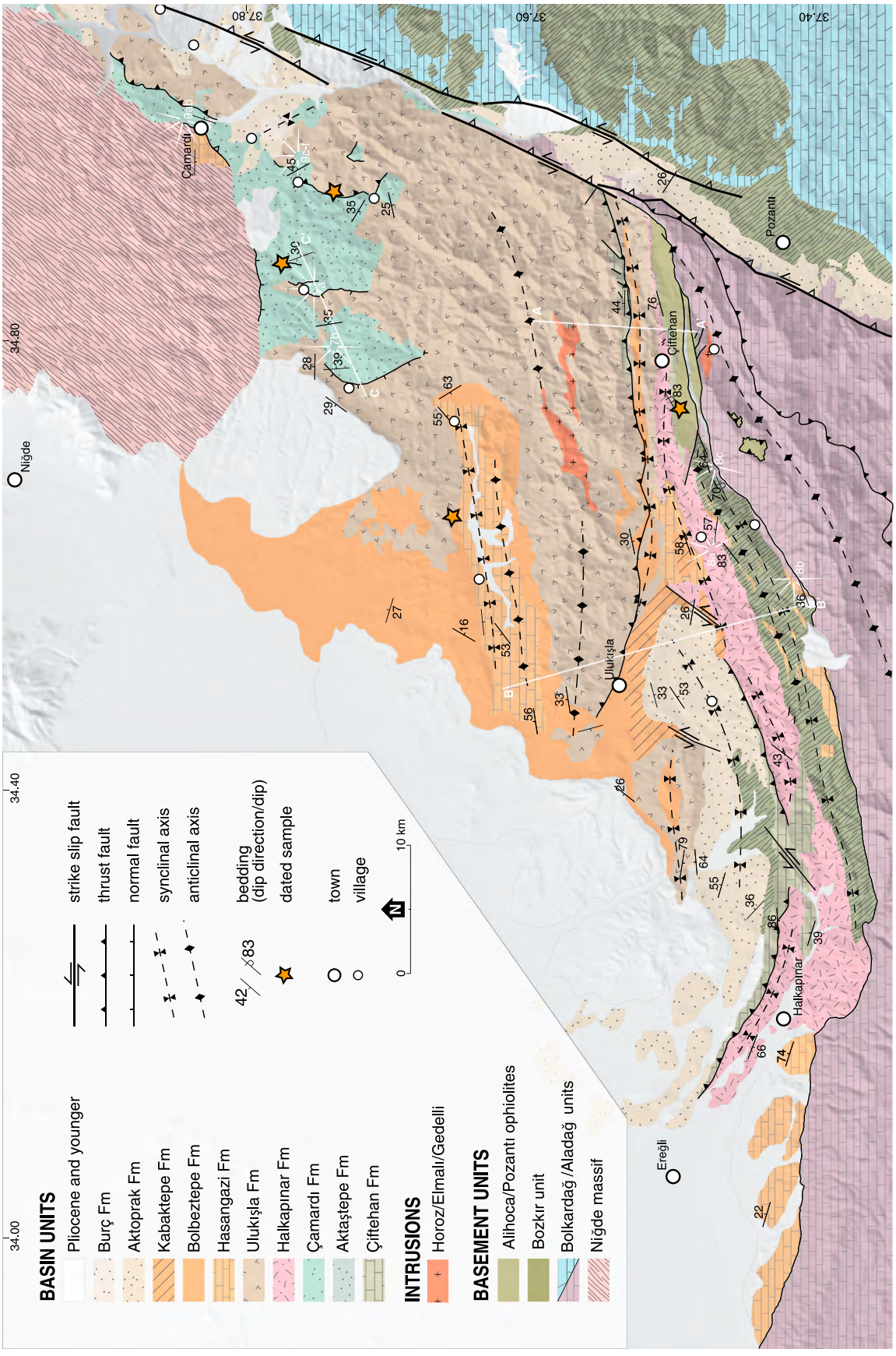

Figure 2. Geological map of the Ulukışla basin and surroundings, modified after existing geological maps (1:100 000 scale [*Atabey et al.*, 1990; *Ulu*, 2009; *Alan et al.*, 2011a, 2011b; *Clark and Robertson*, 2002, 2005]). The map shows major folds and fault zones, bedding attitudes projected onto a digital elevation model. The locations of cross-sections A-A', B-B', C-C' (Figure 6), and of field photographs are indicated. Geochronology sampling localities are marked by orange stars.

Relics of this plate are preserved as ophiolites throughout Turkey (Figure 1). Anatolia is our case study area where we aim to develop a conceptual model to deduce the plate motion history of a former plate—that no longer exists—relative to its former plate boundaries from the geological record contained in the Ulukışla basin (Figure 2). To this end, we study the intense deformation and deposition history of this basin that formed on the southern leading edge of the overriding oceanic plate preserved as the Alihoca suprasubduction zone ophiolite [*Dilek et al*., 1999], above the coevally active southern subduction zone. This basin contains a long and well-exposed time-rock archive since its formation in the Late Cretaceous [*Dilek et al*., 1999; *Clark and Robertson*, 2002, 2005] and provides structural and temporal constraints on the tectonic evolution of the Alihoca ophiolite. We will use this information, in combination with published constraints on the tectonic evolution of Central Anatolia, to deduce the motion history of the Neotethyan Anadolu oceanic plate and its surrounding trenches relative to Africa and Eurasia, and to estimate the convergence history between the two north dipping Anatolian subduction systems, until the demise of the northern one.

2. Geological Setting

2.1. Formation of Anatolian Tectonic Collage

The complex geological history of Anatolia has long been recognized to result from the interaction of multiple subduction zones in space and time, consuming oceanic and continental lithosphere and accommodating Africa-Eurasia convergence [e.g., *Şengör and Yılmaz*, 1981; *Robertson and Dixon*, 1984]. Since the Late Cretaceous, sedimentary and crystalline rocks were scraped off from subducting continental fragments and intervening Neotethyan Ocean basins, forming Anatolia (Figure 1). The resulting ~E-W trending orogen comprises a tectonic collage of intensely deformed, in part metamorphosed and intruded rock units. The northern part of the orogen comprises the Pontides (Figure 1), an amalgamation of Paleozoic crystalline basement derived from the Gondwana margin, overlain by a Mesozoic and younger volcano-sedimentary cover. The Pontides have been part of Eurasia since at least early-mid Mesozoic time [*Şengör and Yılmaz*, 1981; *Ustaömer and Robertson*, 1997, 2010; *Okay and Nikishin*, 2015]. The Pontides are bordered in the south by the Izmir-Ankara-Erzincan (IAE) suture zone, a mélange zone widely thought to represent a fossil subduction zone that consumed oceanic lithosphere of the Neotethys Ocean (Figure 1) [*Şengör and Yılmaz*, 1981]. This suture forms the root zone of a wide belt of ophiolites, that is a roof thrust above continent-derived units collectively referred to as the "Anatolide-Taurides." The leading edge of the Anatolide-Tauride continental margin underwent high-pressure-low-temperature (HP-LT) metamorphism [*Candan et al*., 2005; *Pourteau et al*., 2010, 2013], with progressively younger ages of accretion and metamorphism from north to south [*Göncüoglu*, 1997; *Okay and Tüysüz*, 1999; *van Hinsbergen et al*., 2016]. The timing of formation of the ophiolites is obtained by dating metamorphic soles or plagiogranites from the ophiolite complex and ranges between 89 and 94 Ma [*Dilek et al*., 1999; *Parlak and Delaloye*, 1999; *Önen and Hall*, 2000; *Çelik et al*., 2006, 2011; *van Hinsbergen et al*., 2016]. Metamorphic soles are interpreted to have formed shortly after the initiation of the southern subduction system [e.g., *Stern et al*., 2012; *van Hinsbergen et al*., 2015]. A spreading center must have existed in the overriding oceanic lithosphere above the southern subduction zone, close to the trench [*van Hinsbergen et al*., 2016], as suggested by the suprasubduction zone (SSZ)-geochemical signature of these ophiolites [*Yaliniz et al*., 1996, 2000a, 2000b; *Yaliniz and Göncüoglu*, 1998; *Dilek et al*., 1999; *Parlak et al*., 2000; *Yaliniz*, 2008]. For a comprehensive review on the geochronology of the ophiolites of the Tauride belt and Central Anatolia the reader is referred to *Parlak et al*. [2013] and *van Hinsbergen et al*. [2016].

Overlying these ophiolites are numerous sedimentary basins forming the Central Anatolian basin system (including the Haymana, Tuzgölü, Ulukışla, and Sivas basins; Figure 1) [e.g., *Görür et al*., 1984, 1998; *Koçyigit*, 1991; *Clark and Robertson*, 2002, 2005; *Gürer and Aldanmaz*, 2002; *Nairn et al*., 2012]. The different interpretations for the origin of the Central Anatolian basin system are mainly due to varying interpretation of the geochemical signatures of volcanic products, and the complex multistage deformation recorded in these basins. In a recent synthesis, *Nairn et al*. [2012, and references therein] suggested that all of the Central Anatolian basins may have different dimensions and different tectonic evolutions, but formed in an extensional setting somehow associated with the subduction of oceanic crust during the latest Cretaceous, followed by regional compression in Paleogene times. These sedimentary basins are located overlying relics of a former Neotethyan oceanic plate preserved as ophiolites [*Görür et al*., 1984, 1998; *Kadioglu et al*., 2006; *Robertson et al*., 2009].

The northernmost of the Central Anatolian basins, the Haymana basin (Figure 1), is interpreted to be a fore-arc basin [e.g., *Görür et al*., 1984], which developed above a Mesozoic accretionary wedge as well as the basement of the Pontide distal margin [*Görür et al*., 1984, 1998; *Okay et al*., 2001; *Nairn et al*., 2012], and therefore is not included in our comparison. Toward its south, the other Central Anatolian basins formed above ophiolites overlying the Anatolide-Tauride distal margin. The Tuzgölü basin (Figure 1) evolved coevally with the Haymana basin during the Late Cretaceous to Eocene [*Görür et al*., 1984]. It has been interpreted as a fore-arc basin [*Görür et al*., 1984] or as a postcollisional extensional/transtensional basin [*Göncüoglu et al*., 1992; *Çemen et al*., 1999]. The development of the Tuzgölü basin has been attributed to movement along an extensional detachment fault in Late Cretaceous times [*Çemen et al*., 1999], owing to the regional exhumation of the Kırşehir block (Figure 1) to its east. Additionally, Late Cretaceous-Paleocene extension in the Tuzgölü, and other Central Anatolian basins, is indicated by surface and subsurface evidence [*Ünadan and Yüksel*, 1978].

In its eastern continuation, the Tuzgölü basin passes into the Ulukışla basin, which is the focus of this study (Figure 1). It was previously classified as an intra-arc basin [*Oktay*, 1982; *Görür et al*., 1998]. Based on facies observations, geochemistry [*Oktay*, 1973; *Clark and Robertson*, 2002; *Alpaslan et al*., 2006; *Kurt et al*., 2008], and subsidence curves; *Clark and Robertson* [2002, 2005] suspected extension during the development of the Ulukışla basin.

In the eastern continuation of the Ulukışla basin, and offset by the Ecemiş fault (Figure 1), the Sivas basin is a ~E-W elongate contraction-dominated basin [*Poisson et al*., 1996, 2016; *Dirik et al*., 1999; *Yılmaz and Yılmaz*, 2006] located between the Tauride fold-thrust belt to the south, the Pontides to its north, and the Kırşehir block to its west (Figure 1). The initial tectonic setting of this basin is a matter of debate [*Poisson et al*., 1996; *Kergaravat et al*., 2016, and reference therein] as outcrops of latest Cretaceous-Paleocene are scarce, but thermal relaxation and fault-controlled subsidence have been invoked [*Dirik et al*., 1999]. Especially, contractional structures in Paleocene-Eocene marine strata of the Sivas basin are well exposed, where they are incorporated into a fold and thrust belt.

The study of the early stages of most of the Central Anatolian basins is complicated by erosion and postcollisional cover. As the Ulukışla basin, however, is exceptionally well exposed [*Clark and Robertson*, 2002], we study it to unravel the early tectonostratigraphic evolution of deformation associated with and close to the southern Anatolian subduction zone.

2.2. Regional Evolution of the Basement of the Ulukışla Basin

The northernmost and oldest accreted rocks below the Anatolian ophiolites belong to the Kırşehir block (Figure 1). These dominantly consist of meta-carbonates, and subordinate clastic sediments of continental origin that were underthrusted below ophiolites by ~85 Ma [*Yaliniz and Göncüoglu*, 1998; *Yaliniz et al*., 2000a; *Whitney and Hamilton*, 2004], experienced regional HT/M-LP metamorphism peaking at 700–800°C and 6–8 kbar, and were subsequently overprinted by a local reheating event at lower pressures (2–4 kbar) [*Kocak and Leake*, 1994; *Whitney et al*., 2001; *Whitney and Hamilton*, 2004; *Gautier et al*., 2008; *Lefebvre et al*., 2015]. The Kırşehir block (Figure 1) was intruded by arc granitoids at ~85–70 Ma [*Yaliniz et al*., 1999; *Kadioglu et al*., 2003, 2006; *Köksal et al*., 2012]. During and after granitoid intrusion, it underwent thinning and exhumation, with $^{40}Ar/^{39}Ar$ cooling ages clustering between ~80 and 65 Ma [e.g., *Kadioglu et al*., 2003; *Whitney et al*., 2003; *Gautier et al*., 2008; *Isik et al*., 2008; *Boztuğ et al*., 2009, 2009a, 2009b; *Idleman et al*., 2014; *van Hinsbergen et al*., 2016].

A restoration of Central Anatolia based on vertical axis rotations recovered from paleomagnetic data from the granitoids in the Kırşehir block argued for the existence of a prominent N-S striking segment in the intraoceanic subduction zone west of this block [*Lefebvre et al*., 2013]. This added geometric complexity in the southern subduction system is here termed as the "Kırşehir segment." Shear zones formed during exhumation and detachment faults across the Kırşehir block (Figure 1) show that exhumation was associated with E-W extension [*Gautier et al*., 2008; *Isik et al*., 2008; *Isik*, 2009; *Lefebvre et al*., 2011, 2015], when corrected for Cenozoic vertical axis block rotations [*Lefebvre et al*., 2013]. Sedimentary basins overlying the Kırşehir block (Figure 1) show that E-W extension stopped prior to the mid-Eocene (Lutetian) and was followed by N-S shortening in late Eocene and younger time [*Gülyüz et al*., 2013; *Advokaat et al*., 2014]. The southernmost part of the Kırşehir block, the Niğde massif (Figure 1), has undergone multiple cycles of

burial and exhumation [*Umhoefer et al*., 2007; *Whitney et al*., 2007, 2008; *Idleman et al*., 2014]. Structural studies have identified a top-to-the-NE detachment (present-day orientation) between ophiolites and metamorphic rocks in the Niğde massif [*Gautier et al*., 2002, 2008]. Cooling of these rocks at 75–70 Ma was probably related to tectonic exhumation [*Whitney et al*., 2003, 2007; *Umhoefer et al*., 2007; *Gautier et al*., 2008; *Idleman et al*., 2014], consistent with regional constraints from the Kırşehir block [*van Hinsbergen et al*., 2016, and references therein]. *Gautier et al*. [2002, 2008] and *Umhoefer et al*. [2007] observed that the original contact at the eastern and southern margins between Ulukışla basin sediments and the underlying basement is an unconformity overlain by lower Eocene nummulitic limestones. Therefore, the initial unroofing of the Niğde massif is interpreted as pre-Eocene [*Gautier et al*., 2002, 2008], partly accommodating the pre-Eocene sedimentation in the Ulukışla basin. *Idleman et al*. [2014] inferred that Oligocene reburial of the eastern margin of the Niğde massif resulted in a thermal reheating event that is observed by sub-greenschist facies metamorphism of these Eocene sediments. This reburial was attributed to transpressional movement along the Ecemiş fault [*Koçyiğit and Beyhan*, 1998; *Jaffey and Robertson*, 2001], bounding the massif to the east. The above described contact between basement and sediments was deformed again as a low-angle, intensely sheared fault zone, leading to renewed extensional exhumation of the Niğde massif sometime after the Eocene. Fission track ages suggest that this second stage of exhumation occurred in Miocene time [*Fayon et al*., 2001]. A high-angle normal fault presently separates the southern margin of the Niğde massif from Ulukışla basin sediments (Figures 2, 5, and 7a) [*Toprak and Göncöoğlu*, 1993; *Whitney and Dilek*, 1997; *Clark and Robertson*, 2002; *Gautier et al*., 2002, 2008]. This fault was originally interpreted as detachment [*Whitney and Dilek*, 1997, 1998; *Fayon et al*., 2001; *Whitney et al*., 2001], but more likely corresponds to a late normal fault that was active after the Niğde massif was unroofed a second time [*Gautier et al*., 2002, 2008].

To the south of the Kırşehir block, the ~E-W trending Taurides (Figure 1) developed at the passive margin of Gondwana, and later, together with their passive distal margin (Tavşanlı and Afyon zones) were incorporated into a thin-skinned fold-thrust belt in latest Cretaceous until at least Eocene time [*Monod*, 1977; *Gutnic et al*., 1979; *Demirtasli et al*., 1984; *Özgül*, 1984]. The Tauride fold-thrust belt is subdivided into four zones [*Özgül*, 1984]. The structurally lowest, youngest nappes are the Aladağ and Geyikdağ zones, comprising Paleozoic-Mesozoic platform carbonates. The Bozkır unit corresponds to the previously mentioned ophiolites, associated mélange with large limestone blocks. The underlying Bolkardağ nappe comprises platform-margin sediments, which in many places underwent HP-LT metamorphism (6–9 kbar, ~350°C [*Candan et al*., 2005; *Pourteau et al*., 2010, 2014] to 13–14 kbar/400°C [*Rimmelé et al*., 2005]). Where metamorphosed, the Bolkardağ nappe is also known as Afyon zone. Cooling of the Afyon zone is dated by $^{40}Ar/^{39}Ar$ geochronology on phengite at 67–62 Ma, suggesting peak metamorphism slightly before 70 Ma [*Özdamar et al*., 2013; *Pourteau et al*., 2013].

A widely held view is that the ophiolites thrust upon the Tauride fold-thrust belt, including the Alihoca ophiolite underlying the Ulukışla basin, root in and formed as a result of intraoceanic subduction in an "Intra-Tauride Ocean" [*Şengör and Yılmaz*, 1981; *Görür et al*., 1984] in between the Kırşehir block and the Tauride platform, including the Afyon zone [*Görür et al*., 1984; *Dilek et al*., 1999; *Okay and Tüysüz*, 1999]. As already pointed out by *Poisson et al*. [1996], and recently further explained by *van Hinsbergen et al*. [2016], there is no kinematic need for such an extra subduction zone forming at ~95 Ma within the Intra-Tauride Ocean in addition to the one within the Neotethys north and east of the Kırşehir block: the ophiolites overlying the Kırşehir block as well as the Taurides can straightforwardly be explained as an originally coherent overriding oceanic plate that became underthrusted and accreted by a southward and westward foreland propagating fold-thrust belt [*van Hinsbergen et al*., 2016]. An "Intra-Tauride basin" (Figure 11), however, may well have existed: subduction below and following the accretion of the Kırşehir block below the ophiolite sheet between 85 and 70 Ma was associated with the formation of a volcanic arc within the Kırşehir block [*Kadioglu et al*., 2003; *Ilbeyli et al*., 2004, 2009; *Ilbeyli*, 2005; *Delibaş and Genc*, 2012; *Köksal et al*., 2013], while no rocks accreted below the Kırşehir block at this time. This subduction episode may have consumed oceanic crust, but there is no known geological record of this to date [*van Hinsbergen et al*., 2016].

To the south of the Ulukışla basin, the deepest structural units are those of the nonmetamorphic Tauride carbonate platform (Figure 1), overlain by the metasediments of the Bolkardağ unit, which is structurally overlain by ophiolite and ophiolitic mélange of the Bozkır unit. Ophiolite and mélange are unconformably overlain by Ulukışla basin sediments (Figures 2 and 3). The SSZ signature of the Alihoca ophiolite [*Dilek et al*., 1999] places

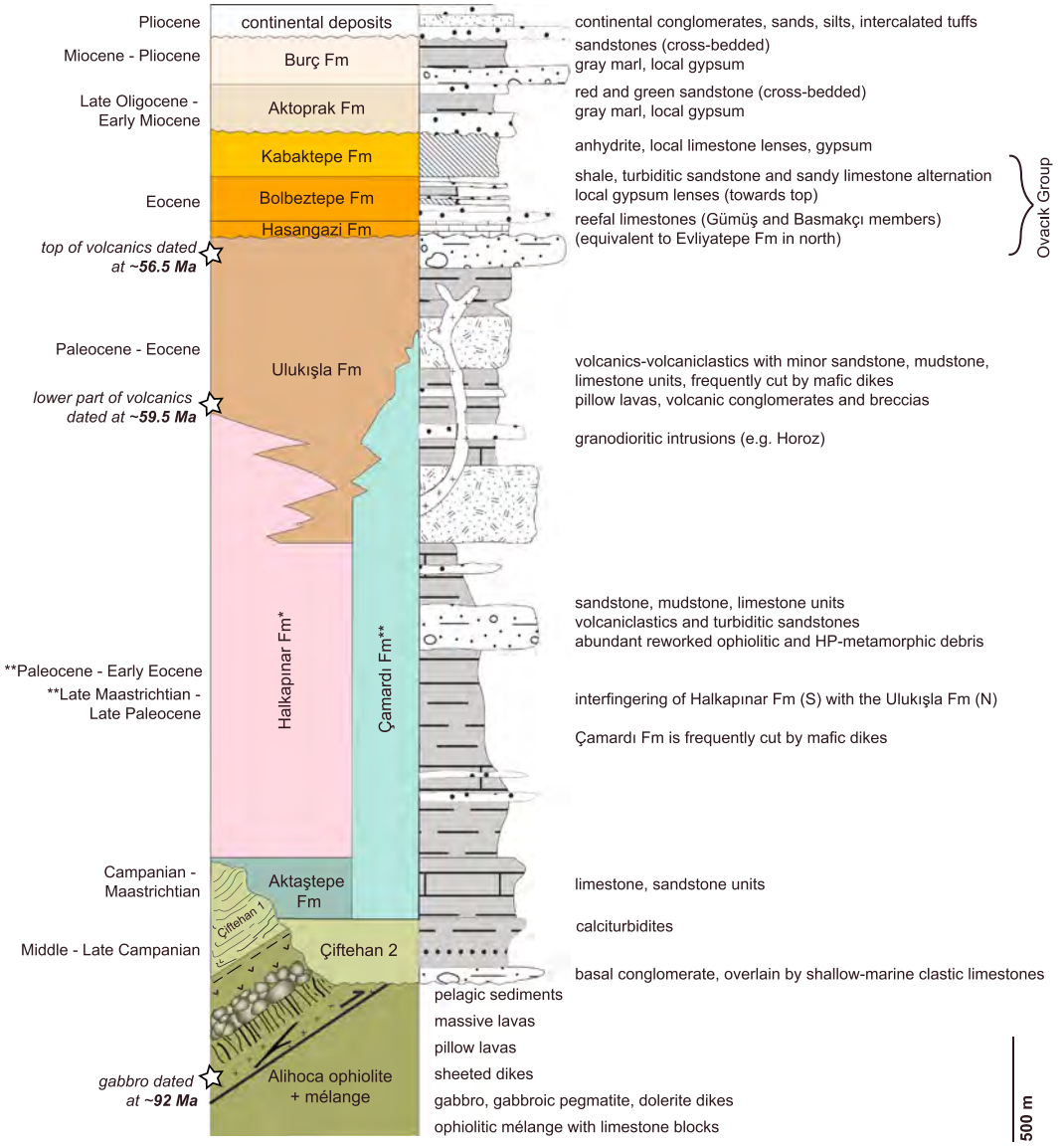

Figure 3. Generalized lithostratigraphic column of the Ulukışla basin.

its formation close to the trench. At the northern entrance to the village of Alihoca, serpentinized peridotites, pyroxenites, ultramafic cumulates, layered gabbros, sheeted dikes, and radiolarites are found. Hornblende from a mafic dike yielded an $^{40}Ar/^{39}Ar$ age of 90.8 ± 0.8 Ma [*Dilek et al.*, 1999].

Following accretion, metamorphism, and exhumation of the Kırşehir block and the Afyon zone, and the accretion of the Tauride nappes, the Central Anatolian orogen underwent renewed crustal thickening and regional N-S shortening. This started when the Kırşehir block collided with the Pontides, leading to oroclinal bending of the latter in the Paleogene [*Meijers et al.*, 2010], and was associated with contractional deformation, lasting until the early Miocene, as observed for instance in the Çankırı basin [*Kaymakci et al.*, 2003, 2009]. The Kırşehir block broke into three blocks that underwent differential vertical axis rotations [*Lefebvre et al.*, 2013], accommodated along fold-thrust zones with possible strike-slip components [*Gülyüz et al.*, 2013; *Lefebvre et al.*, 2013; *Advokaat et al.*, 2014]. Together, these thrusts may have accounted for several hundred kilometers of latest Cretaceous to earliest Miocene shortening taken up in the buffer zone of the Africa-Eurasia convergence. The rest of this convergence is accommodated in a subduction zone that is at present located just south of Cyprus and remains active today [*Reilinger et al.*, 2010].

The contact between the Afyon/Bolkardağ zone and the Kırşehir block is not exposed in outcrops, being covered by Upper Cretaceous-Cenozoic sediments (Figure 1), which have also recorded the timing and style of surface deformation during the exhumation of both units. The best exposed and chronostratigraphically most complete basin that separates and covers these basement units is the Ulukışla basin (Figure 2). Its sediments range from Upper Cretaceous to Quaternary in age (Figure 3) and are found in unconformable or faulted contact with ophiolite or ophiolitic mélange, with the Niğde massif that forms the southernmost part of the Kırşehir block, and with the Afyon/Bolkardağ zone. Therefore, the Ulukışla basin is an ideal place to study the mechanics of exhumation of the Niğde massif and the associated kinematics at the contact between the Afyon zone and the Niğde massif.

2.3. Architecture of the Ulukışla Basin

The Ulukışla basin (Figure 2) comprises a stratigraphically discontinuous and laterally variable series of continental coarse clastic rocks, shallow and deeper marine clastic, and carbonate sediments interlayered with volcanic rocks. The deposits overlie the ophiolitic basement and metamorphic rocks of the Niğde massif at the southern part of the Kırşehir block and those of the Afyon/Bolkardağ zone.

Significant deformation has affected the southern part of the basin, resulting in widely exposed subvertical to overturned stratigraphy oriented ~E-W. Westward this zone becomes wider and structures become gradually NE-SW oriented, while several open synclines deform the base stratigraphy of the basin. In this part of the basin, the subvertical position of the Cretaceous-Paleogene strata was related to large-scale (drag-) folding interpreted as an effect of backthrusting of the Bolkardağ unit over the Ulukışla basin [*Blumenthal*, 1956; *Demirtaşlı et al*., 1973] although the kinematics of such a back thrust remain unclear.

In the east, the Ulukışla basin sediments are demarcated by the Ecemiş fault zone (Figures 2, 5, and 8), which is a ~60–80 km offset sinistral shear zone that truncates the Bolkardağ metamorphic rocks and the Aladağ Mountains, part of the Tauride nappe system [*Yetis*, 1984; *Jaffey and Robertson*, 2001, 2005]. Based on biostratigraphic age dating of sediments affected by the fault, *Yetis* [1984] interpreted that the bulk of this displacement occurred between the Paleocene and Lutetian, whereas structural and stratigraphic evidence [*Jaffey and Robertson*, 2001, 2005] suggest that most of the strike-slip displacement occurred between 13 and 5 Ma. To the south of the study area, lower Miocene sediments essentially seal the Ecemiş fault in the Adana basin and are only subtly deformed [*Jaffey and Robertson*, 2001; *Alan et al*., 2011a; *Higgins et al*., 2015; *Sarıkaya et al*., 2015]. These studies have also inferred that the fault zone experienced E-W directed normal faulting with a minor strike-slip component since the latest Miocene-early Pliocene.

To the west, the Upper Cretaceous to Paleogene stratigraphy is covered by upper Neogene sediments and volcanic rocks of the Tuzgölü basin and reappears in narrow slivers along the eastern margin of the Tuzgölü basin [*Görür et al*., 1984].

3. Stratigraphy

The lithostratigraphy of the Ulukışla basin (Figure 3) described below integrates previous studies [*Blumenthal*, 1956; *Ketin and Akarsu*, 1965; *Oktay*, 1982; *Demirtaşlı et al*., 1973; *Oktay*, 1973, 1981; *Demirtasli et al*., 1984; *Atabey et al*., 1990; *Görür et al*., 1998; *Clark and Robertson*, 2002, 2005] with our new field observations and biostratigraphic data. The ages assigned to the sedimentary units are based on previous micropaleontological data [*Demirtasli et al*., 1984], complemented with new sampling for biostratigraphic dating in key locations using benthic and planktonic foraminifera and calcareous nannofossils.

3.1. Lithostratigraphy and Biostratigraphy

The oldest sediments unconformably overlying the ophiolites and ophiolitic mélange, and associated deepwater sediments in the southern part of the Ulukışla region, comprise a series of deep marine red clays, limestones, and clastic rocks, previously included in the *Çiftehan Formation* (Figure 3) [*Demirtasli et al*., 1984]. These ~80 m thick sediments are exposed along a road section in the southern part of the basin (near Ardıçlı village; Figure 2). Other laterally continuous exposures of variable thickness are found near Çiftehan, Alihoca, and Maden villages. Our field observations show that the sediments of this formation are composed of two different packages that infer two different depositional settings. Overlying the ophiolites, ophiolitic mélange, and associated red deepwater shales and radiolarites conformably, the first package (Çiftehan 1; Figure 3) is composed of calciturbidites containing clasts of ophiolitic material that grade upward in the

stratigraphy into red pelagic limestones, finely laminated siltstones and thin turbiditic sandstones. These sediments are affected by significant deformation and pervasive cleavage. The second sedimentary package is deposited over an erosional unconformity and is composed of conglomerates overlain by shallow-marine clastic limestones that elsewhere in the center of the basin grade to sandstones, deeper water limestones, and calciturbidites. This second sedimentary package (Çiftehan 2; Figure 3) is generally defined as deposited in the Ulukışla basin, implying that the first package (Çiftehan 1) represents a remnant of a sedimentary sequence deposited on the ophiolites and their mélange during their uplift phase that predated the onset of shallow-marine Ulukışla basin sedimentation. Planktonic foraminifera and nannofossils from the first package, the red pelagic limestones, give a Campanian age (samples BS4a–BS4d and sample AL1 in the supporting information). Planktonic foraminifera and nannofossils of the sandstones overlain by calciturbidites of the second sedimentary package in the center of the basin (BS20 location in the supporting information) indicate an early Campanian to early Maastrichtian depositional age. These observations show that the onset of sedimentation took place during Campanian-Early Maastrichtian over an erosional unconformity in the basin center, while the southern margin of the basin recorded coeval sedimentation on top of the accretionary wedge (Figure 3). Therefore, we propose to exclude the first package from the stratigraphy of the Ulukışla basin (i.e., from the Çiftehan Formation).

The *Aktaştepe Formation* (Figure 3) is observed only near the southern margin of the basin, where it unconformably overlies the ophiolites, their mélange, and the first sedimentary package of the Çiftehan Formation (Figure 3). The Aktaştepe Formation has several members [*Clark and Robertson*, 2002, 2005] that were previously defined as formations [e.g., *Demirtasli et al*., 1984] and has a thickness of ~300 m. In the Ardıçlı road section the Aktaştepe Formation is only 10 m thick and consists of a coarse conglomerate with limestone matrix that grades into limestones. Benthic foraminifera suggest a Campanian-Maastrichtian age (sample BS5 in the supporting information). According to *Clark and Robertson* [2002, 2005] limestone pebbles in coarse conglomerates in the Alihoca valley were derived from the Bolkar carbonate platform as well as from the ophiolitic mélange. The most spectacular outcrop of the Aktaştepe Formation is the major vertical to overturned Kalkankaya cliff west of Alihoca village (Figure 8b), the base of which we dated as Late Campanian-Early Maastrichtian (sample BS6B in the supporting information).

The *Halkapınar Formation* (Figure 3) conformably overlies the Aktaştepe Formation and is overlain by volcanic rocks of the Ulukışla Formation. Where the Ulukışla Formation is absent, the Hasangazi Formation unconformably overlies the Halkapınar Formation, which consists of conglomeratic sandstones grading into a sandstone-siltstone sequence. Blocks of HP-metamorphic rocks and recrystallized limestone are common. A representative succession of this formation can be found south of Gümüş village (Figure 6). The age assigned to this formation is middle Paleocene-early Eocene [*Demirtasli et al*., 1984] or late Maastrichtian-late Paleocene [*Clark and Robertson*, 2002]. Nannofossils yielded an age interval spanning the late early-early late Paleocene to late Paleocene-early Eocene (sites AL2, HP1, and HP6 in the supporting information). The thickness of the formation is at least 1000 m [*Demirtasli et al*., 1984] and may be as thick as 2000 m in the west [*Clark and Robertson*, 2005].

In the northern part of the basin, the *Çamardı Formation* (Figure 3) is the oldest and contains conglomerates and overlying detrital rocks. Some authors defined the Eskiburç group within the Çamardı Formation, which would be of volcanic nature with a late Paleocene age [*Yetiş et al*., 1995]. Others suggested a Maastrichtian age [*Demirtasli et al*., 1984; *Göncüoglu et al*., 1991]. We have only observed dikes cutting the Çamardı Formation and cannot confirm Maastrichtian volcanism in the Ulukışla region. We consider the Eskiburç group, interfingering with the Çamardı Formation, as the basal part of the Ulukışla Formation. The formation here referred to as the Çamardı Formation was interpreted as the postvolcanic, Eocene Bolbeztepe Formation by *Clark and Robertson* [2002, 2005]. Our new observations show instead that the Çamardı Formation rocks underlie and interfinger with the Ulukışla Formation volcanics. This is in agreement with our new paleontological data (nannofossils) indicating Late Cretaceous to late Paleocene (Thanetian) ages, progressively younging from west to east (samples PC1, PC2, PC3, PC4, BU1, and BU2 in the supporting information), confirming earlier findings [*Göncüoğlu*, 1986; *Göncüoglu et al*., 1991]. The deposition of the Çamardı Formation was indeed coeval with the deposition of the Aktaştepe and Halkapınar Formations in the southern part of the basin. The formation has a thickness of several hundreds of meters, but because no contact with its basement has been observed, it may be thicker. In most places the Çamardı Formation is unconformably overlain by the terrestrial redbeds of Oligocene-early Miocene age or by limestones of the lower to middle Eocene

AGU Tectonics

10.1002/2016TC004206

Table 1. Zircon U-Pb Data of Magmatic Units From the Ophiolitic Basement and Volcanic Infill of the Ulukışla Basin

Properties	Weight	U	Th/U	Pbc	206/204	207/235	2 sigma	206/238	2 sigma	rho	207/206	2 sigma	206/238	2 sigma	207/235	2 sigma
	(μg)	(ppm)		(pg)			(abs)		(abs)			(abs)	(Ma)	(abs)	(Ma)	(abs)
a	b	b	c	d	e	f	f	f,g	f	f	f,g	f	f,g	f	f	f
UK1.1 (Lat 37.500298°, Long 34.727940°)																
UK2013-1.1 388/61 ZIR	2	461	0.28	2.0	339	0.09659	0.00239	0.014504	0.000049	0.48	0.0483	0.0011	92.83	0.31	93.63	2.21
UK2013-1.1 388/60 ZIR	26	4792	0.50	1.0	116303	0.09507	0.00031	0.014411	0.000043	0.97	0.0478	0.0000	92.23	0.28	92.22	0.29
UK2013-1.1 388/62 ZIR	13	1065	0.79	2.5	5010	0.09508	0.00028	0.014394	0.000030	0.79	0.0479	0.0001	92.13	0.19	92.23	0.26
UK94 (Lat 37.741280°, Long 34.926479°)																
UK2013-94 388/52 ZIR	6	1028	1.58	2.8	1289	0.06086	0.00034	0.009301	0.000020	0.53	0.0475	0.0002	59.68	0.13	59.99	0.32
UK2013-94 388/53 ZIR	6	886	1.91	6.7	483	0.06131	0.00064	0.009315	0.000030	0.48	0.0477	0.0004	59.77	0.19	60.42	0.61
UK9.4 (Lat 37.779083°, Long 34.863605°)																
UK2013-9.4 390/13 ZIR	19	495	1.54	4.1	1360	0.06077	0.00026	0.009315	0.000019	0.61	0.0473	0.0002	59.77	0.12	59.90	0.25
UK2013-9.4 388/59 ZIR	7	363	0.84	5.1	306	0.06095	0.00084	0.009283	0.000023	0.38	0.0476	0.0006	59.57	0.15	60.07	0.81
UK2013-9.4 390/14 ZIR	9	368	1.05	3.0	648	0.06012	0.00060	0.009243	0.000043	0.58	0.0472	0.0004	59.31	0.27	59.28	0.58
UK5.1 (Lat 37.662159°, Long 34.635841°)																
UK2013-5.1 388/56 ZIR	11	298	1.26	16.3	130	0.05944	0.00168	0.008878	0.000033	0.15	0.0486	0.0014	56.98	0.21	58.63	1.61
UK2013-5.1 388/58 ZIR	36	228	2.66	10.2	463	0.05795	0.00045	0.008862	0.000019	0.36	0.0474	0.0003	56.88	0.12	57.20	0.43
UK2013-5.1 388/55 ZIR	2	786	1.82	1.0	922	0.05790	0.00055	0.008845	0.000028	0.50	0.0475	0.0004	56.77	0.18	57.15	0.53
UK2013-5.1 388/57 ZIR	45	53	1.40	0.9	1465	0.05731	0.00056	0.008789	0.000022	0.32	0.0473	0.0004	56.41	0.14	56.59	0.54

[a] Main features of analyzed zircon. All zircon grains treated with chemical abrasion [*Mattinson*, 2005].
[b] Weight and concentrations are known to better than 10%.
[c] Th/U model ratio inferred from 208/206 ratio and age of sample.
[d] Pbc = total common Pb in sample (initial + blank).
[e] Raw data, corrected for fractionation and spike.
[f] Corrected for fractionation, spike, blank (206/204 = 18.3, 207/204 = 15.555), and initial common Pb (based on *Stacey and Kramers* [1975]); error calculated by propagating the main sources of uncertainty. The U-Pb ratio of the spike used for this work is adapted to 206Pb/238U = 0.015660 for the ET100 solution as obtained with the ET2535 spike at NIGL.
[g] Corrected for 230Th disequilibrium according to *Schärer* [1984] and assuming Th/U magma = 4.

Evliyatepe Formation [*Göncüoglu et al*., 1991; *Gautier et al*., 2002], which corresponds to the Kaleboynu Formation of *Yetiş et al*. [1995], and have been incorporated here in the Hasangazi Formation.

The *Ulukışla Formation* (Figure 3) is a thick volcano-sedimentary sequence comprising volcanic breccias and conglomerates, pillow lavas and massive lavas, fine-grained volcaniclastic material, and minor, local interbedded limestones. It interfingers with and overlies the Çamardı and Halkapınar Formations and is unconformably overlain by the *Hasangazi Formation*. Thickness estimates for the Ulukışla Formation range from 1500 to 2000 m [*Oktay*, 1982; *Çevikbaş and Öztunalı*, 1991], or even more [*Clark and Robertson*, 2005]. Monzo-syenitic (Gedelli and Elmalı) intrusions cut the volcanic pile. Biostratigraphic constraints from underlying and overlying formations place the Ulukışla Formation somewhere in the Paleocene-Eocene. These biostratigraphic constraints have been further refined by our absolute age dating ranging from ~60–57 Ma (section 3.2).

Postvolcanic marine rocks overlying the Ulukışla Formation are subdivided into the *Hasangazi* and *Bolbeztepe* formations (Figure 3). For convenience of displaying the structure of the basin, we have combined these into the *Ovacık Group* (named after their occurrence in the Ovacık syncline). The Hasangazi Formation [*Clark and Robertson*, 2002, 2005] encompasses the Basmakçı member consisting of deep shelf deposits with lower Eocene benthic foraminiferal assemblages (sample BS18 in the supporting information) and the Gümüş member comprising very shallow inner platform nummulitic limestones of Eocene age (sample BS14 in the supporting information). We include the Evliyatepe Formation of similar age and faunal content that was defined close to the contact with the Niğde massif [*Göncüoglu et al*., 1991; *Gautier et al*., 2002] into the Hasangazi Formation. This formation is overlain by and interfingering with the *Bolbeztepe Formation* turbidites and marls [*Demirtasli et al*., 1984]. Toward the top, the Bolbeztepe Formation contains frequent gypsum beds. Its thickness varies between 200 and 600 m. Nannofossil and benthic foraminifera assemblages suggest an early to middle Eocene age (BS18 and TT1 in the supporting information).

The *Kabaktepe Formation* [*Clark and Robertson*, 2002, 2005] (Figure 3) conformably overlies the Ovacık Group and consists of anhydrite, gypsum, dolomite, and sandstone intercalations. Its occurrence is restricted to the area south of Ulukışla. Thickness estimates vary from 200–300 m [*Clark and Robertson*, 2002, 2005] to 600 m [*Demirtasli et al*., 1984]. The age assigned to this formation, based on microfossils found at its base, is late Lutetian [*Demirtasli et al*., 1984].

The *Aktoprak Formation* (Figure 3) unconformably overlies these evaporites and comprises marls and lacustrine limestones at its ~450 m thick base. A Chattian-Aquitanian age is assumed based on gastropods [*Blumenthal*, 1956]. The limestones are overlain by an ~1000 m thick fluvial red-green clastic sandstones and blue-gray marls that are exposed in the core of the Aktoprak syncline. In the north, close to Burç village, an equivalent clastic fluvial succession of sandstones and silts is known as the Çukurbağ Formation. It is overlain by lacustrine deposits of the *Burç Formation* [*Yetiş*, 1968] (Figure 3). The Çukurbağ Formation dominates sedimentation in the Ecemiş corridor. The Aktoprak and Burç Formations are inferred to be of Oligocene-Miocene age [*Jaffey and Robertson*, 2005]. They are unconformably overlain by Pliocene-Quaternary continental conglomerates, sands, and silts with intercalations of tuff deposits correlated to the Cappadocian volcanic province to the north, which has a late Miocene-Pliocene age [e.g., *Innocenti et al*., 1975; *Lepetit et al*., 2014].

3.2. U-Pb Geochronology

Absolute age dating was carried out by U-Pb isotope dilution thermal ionisation mass spectrometry. Zircon grains were extracted by crushing, milling, and separation by means of a Wilfley table and concentrated with a magnetic separator and heavy liquids. Zircon grains were selected under a binocular microscope and subjected to chemical abrasion [*Mattinson*, 2005, 2010] before spiking with a ^{202}Pb-^{205}Pb-^{235}U tracer, dissolution, and mass spectrometry, following the procedure of *Krogh* [1973] with modifications described in *Corfu* [2004]. Whenever there was only a small amount of Pb available, measurements were done with an ion counting secondary electron multiplier. The obtained data were corrected with fractionation factors of 0.1%/amu for Pb and 0.12%/amu for U subtracting blanks of 0.1 pg U and 2 pg Pb, or less when the total common Pb was below that level. The remaining initial Pb was corrected by using compositions calculated with the model of *Stacey and Kramers* [1975]. The data were also adjusted for a deficit of ^{206}Pb due to initial deficiency of ^{230}Th [*Schärer*, 1984], and the tracer was callibrated with reference to the ET100 solution [*Condon et al*., 2015; *McLean et al*., 2015]. Plotting and regressions were done with the Isoplot software package

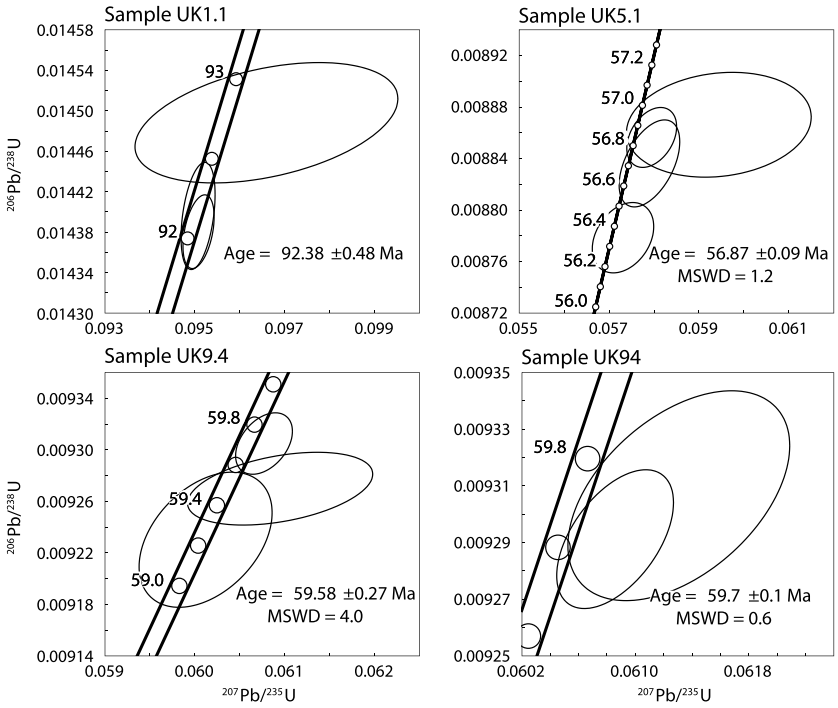

Figure 4. Concordia plots for zircon grains from ophiolitic basement (UK1.1) and volcanic basin units (UK5.1, UK9.4, and UK94). Ellipses indicate the 2σ-uncertainty. MSWD = mean square of weighted deviates.

[*Ludwig*, 2009]. The decay constants are those of *Jaffey et al*. [1971]. Uncertainties in the isotope ratios and the ages are given and plotted at 2σ (Table 1 and Figure 4). Sampling locations can be found in Table 1, on the geological map (Figure 2), and in the stratigraphic column (Figure 3).

A pegmatitic gabbro (UK1.1) from the Alihoca ophiolite was sampled to date the age of ocean floor formation prior to its thrusting onto the Taurides. The sampling locality is in the footwall of the basement-reworking basal conglomerate. The contact between the two units is an erosional unconformity. Three fractions of zircon grains were analyzed (Table 1). The three analyses show some scatter, which may be due some Pb loss of the two fractions containing the highest amount of U (1000 and 4800 ppm). The alternative is that the low U fraction may reflect some earlier zircon growth. The age of 92.38 ± 0.48 Ma, calculated by expanding the errors to reach an acceptable fit, covers both these two possibilities, indicating the time of crystallization of the gabbro.

A welded tuff (UK94) was collected from the base of the of the Ulukışla Formation in the northeastern part of the basin. Zircon grains were predominantly short prismatic to equant with inclusions. Two overlapping analyses yield an average $^{206}Pb/^{238}U$ age of 59.71 ± 0.10 Ma.

A rhyolite (UK9.4) from the lower part of the Ulukışla Formation in the northern part of the basin, offset by N-S trending syn-depositional listric normal faults, was sampled. Zircons in this sample were clear, euhedral prisms, and broken tips with inclusions. Three overlapping fractions yielded a Concordia age of 59.58 ± 0.27 Ma.

Sample UK5.1, is a welded tuff from the top of the volcanic rocks of the Ulukışla Formation in the central western part of the basin, in the northern limb of the Ovacık syncline. It contained mainly prismatic zircon with inclusions. Three of the analyses overlap defining an average $^{206}Pb/^{238}U$ age of 56.87 ± 0.09 Ma. Another analysis is slightly younger, most likely because of some Pb loss.

4. Anisotropy of Magnetic Susceptibility

Strain patterns based on field structural geological constraints may be limited by the quality and extent of the outcrops, and the availability of measurable structures. We therefore use anisotropy of magnetic

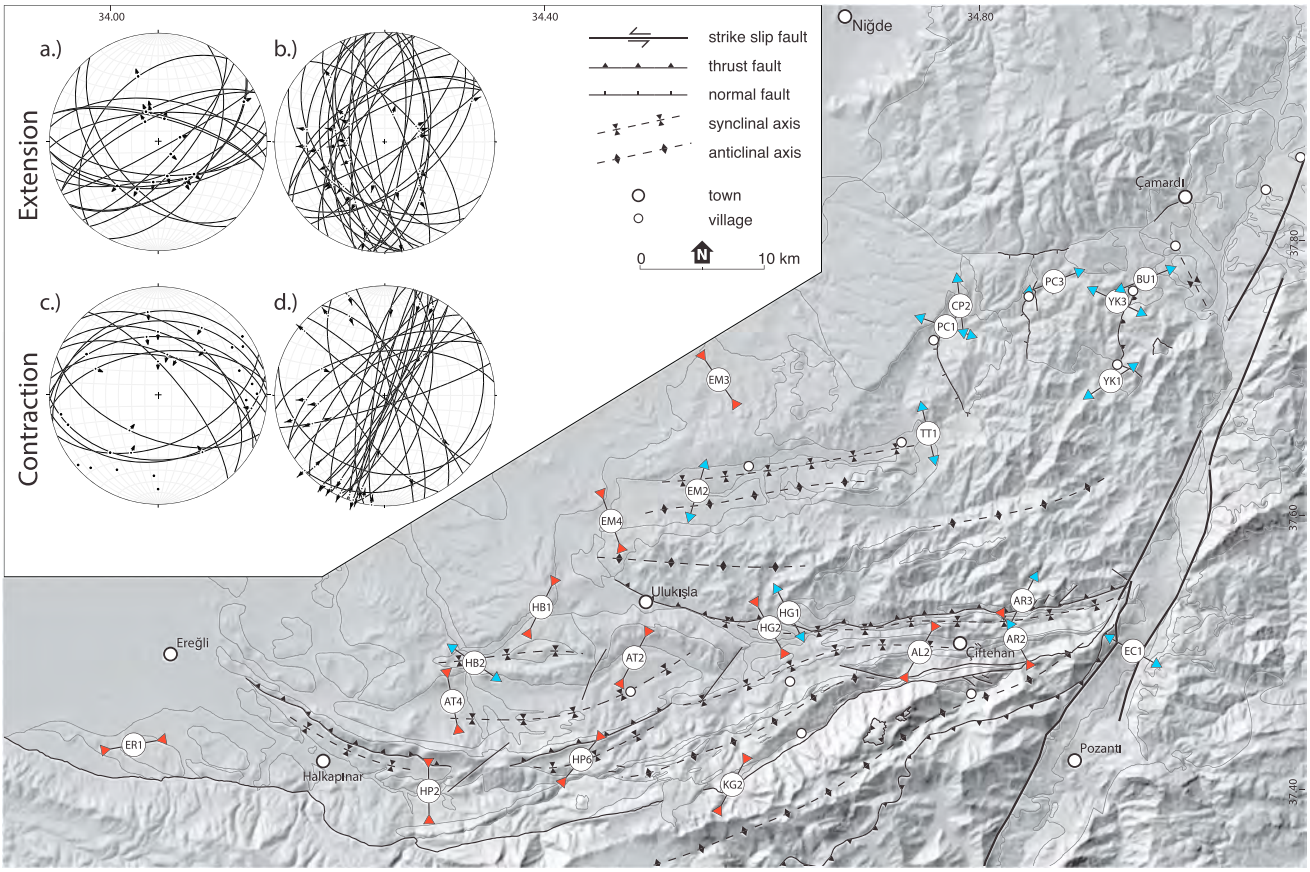

Figure 5. Structural map of the Ulukışla basin showing major structures. AMS sampling localities are marked with circles, fabrics related to extension are marked in blue, and fabrics related to compression are marked in red. Stereoplots (equal area, lower hemisphere) illustrate fault kinematic measurements in basin strata (a) faults related to N-S extension, (b) faults related to E-W extension, (c) faults and folds related to N-S compression, and (d) folds related to E-W compression and strike-slip motion.

susceptibility (AMS) as a complementary tool to our detailed field kinematic analysis and interpret the results on structural grounds. AMS is in fact a powerful tool for petrofabric analyses that may be used to characterize the regional strain evolution in deformed terranes [*Jelinek*, 1977; *Jelínek and Kropáček*, 1978; *Hrouda*, 1982; *Borradaile*, 1988, 1991; *Jackson*, 1991; *Jackson and Tauxe*, 1991; *Rochette et al*., 1992; *Tarling and Hrouda*, 1993; *Parés and van der Pluijm*, 2002; *Soto et al*., 2009; *Maffione et al*., 2015]. With AMS, rock samples can be measured more comprehensively, quickly, and reproducibly than with any other petrofabric technique. AMS reflects the directional variability of magnetic susceptibility as a response to the strain field and provides a way to estimate the shape and direction of the strain ellipsoid. In weakly deformed sediments, AMS reflects the initial fabric produced during incipient deformation at the time of, or shortly after deposition and diagenesis, and therefore has been frequently used in orogenic settings to document the syn-sedimentary tectonic regime [e.g., *Sagnotti and Speranza*, 1993; *Sagnotti et al*., 1998; *Cifelli et al*., 2005; *Soto et al*., 2009; *Maffione et al*., 2012]. AMS fabric analysis complements field observations of the deformation history that is primarily deduced from fault kinematic measurements in combination with growth structures and changes in sedimentary facies.

The axis of maximum magnetic susceptibility (k_{max}; black squares in Figures 7a, 8c, and the supporting information) defines the magnetic lineation (*L*). In sediments affected by weak deformation, the original sedimentary fabric (oblate ellipsoid: $k_{max} \approx k_{int} \gg k_{min}$) is partially overprinted by a tectonic fabric, which results in the development of a triaxial ($k_{max} > k_{int} > k_{min}$) or even prolate ($k_{max} \gg k_{int} \approx k_{min}$) AMS ellipsoid, usually characterized by a well-defined magnetic lineation. With increasing strain, the shape of the AMS ellipsoid progressively modifies from purely oblate ($k_{max} \approx k_{int} \gg k_{min}$), typical of a "sedimentary fabric," to a more "tectonic

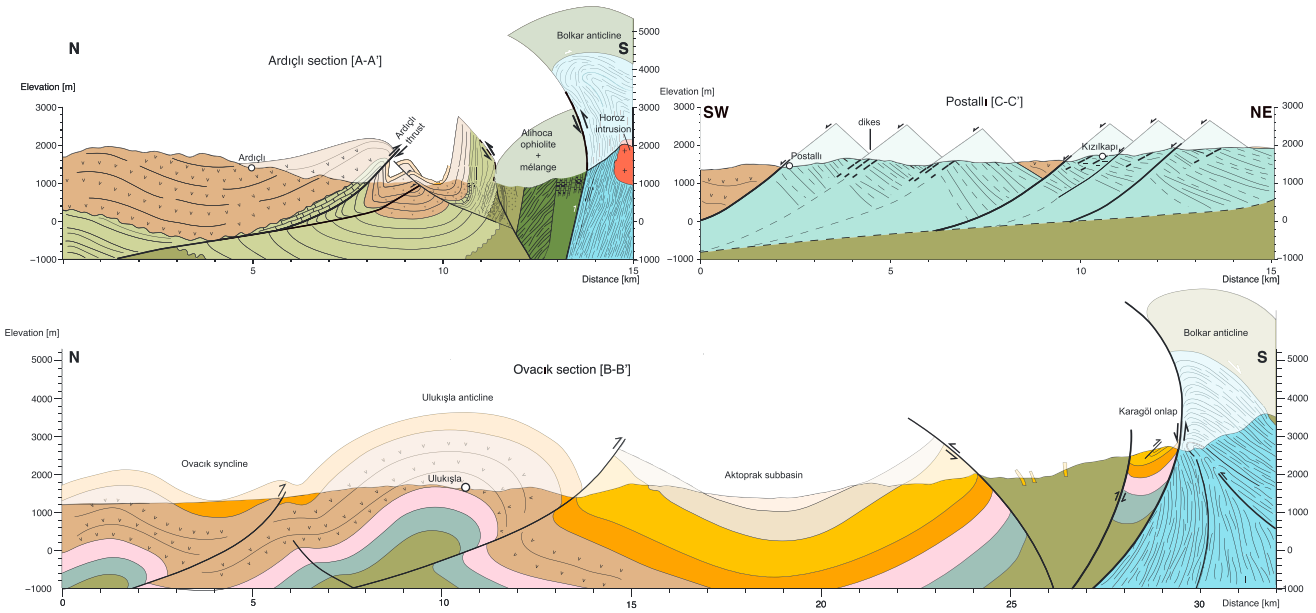

Figure 6. Structural cross sections across the southern (A-A′ and B-B′) and northern (C-C′) basin margins. Locations are marked in the geological map (Figure 2). Formations are equivalent to those in the stratigraphic column (Figure 3).

fabric" (triaxial: $k_{max} > k_{int} > k_{min}$ or prolate: $k_{max} \gg k_{int} \approx k_{min}$). The highest stage of deformation is characterized by the formation of an oblate ellipsoid with the magnetic foliation parallel to the cleavage/schistosity [e.g., *Parés*, 2004].

The relationship between the local attitude of the studied rock and the direction of the magnetic lineation can be used to discriminate between tectonic regimes (compressive versus extensional) [*Mattei et al.*, 1997]. In extensional settings, the magnetic lineation aligns with the stretching direction and the local bedding dip, and hence perpendicular to the orientation of local normal faults. In compressional settings, the magnetic lineation is usually subhorizontal and parallel to both the local strike of the strata and folds axes [e.g., *Mattei et al.*, 1997; *Parés*, 2004; *Maffione et al.*, 2012].

We sampled the entire stratigraphy of the Ulukışla basin ranging from Upper Cretaceous to Miocene-Pliocene. The obtained patterns of preferred orientations of mineral grains result from the interplay of mineral, sedimentary, tectonic, and/or composite fabrics [*Weil and Yonkee*, 2009]. We show our AMS data after tectonic correction (Figures 5, 7, and 8) as the majority of sites are inferred to have acquired their fabric shortly after deposition and before tilting.

The mean susceptibility (k_m) varies between 98.7 and 4380 (10^{-6} SI), with most frequent values at ~800 (10^{-6} SI). The site mean corrected anisotropy degree (P′) is relatively low with all values below 1.120, and ~95% of sites below 1.070 (Table DR2.1 in the supporting information). A purely sedimentary fabric is only recorded at one site (EM1), where the k_{int} and k_{max} axes cannot be clearly resolved and the shape of the AMS ellipsoid is mainly oblate. The remaining 28 sites show a tectonic overprint of the original sedimentary fabric, which resulted in the formation of triaxial to prolate AMS ellipsoids. The majority of the sites ($n = 25$) show oblate-triaxial ($T > 0$) AMS ellipsoids, while the remaining three sites display a prolate ($T < 0$) AMS ellipsoid (Table DR2.1). In the 25 sites showing oblate-triaxial ellipsoids the magnetic foliation plane is subparallel to the strata (the pole to local bedding lies within the distribution of the k_{min} axes; see Figure DR2.1 and Table DR2.1 in the supporting information). This, together with the low values of P′, suggests that the studied units have only been affected by a weak strain.

The mean magnetic lineation is well developed ($e_{12} > 40°$; see Table DR2.1) at 25 sites. Although site PC3_4_CP1 shows a relatively large scatter of the k_{max} ($e_{12} > 40°$), this is mainly due to the combination of three different sites with variable bedding attitude. Within those 25 ellipsoids, the magnetic lineation is subparallel to both the local strike of the units and nearby fold axes at 13 sites, and roughly perpendicular at 12 sites. Adopting criteria used in previous AMS studies [e.g., *Mattei et al.*, 1997], we interpret the magnetic

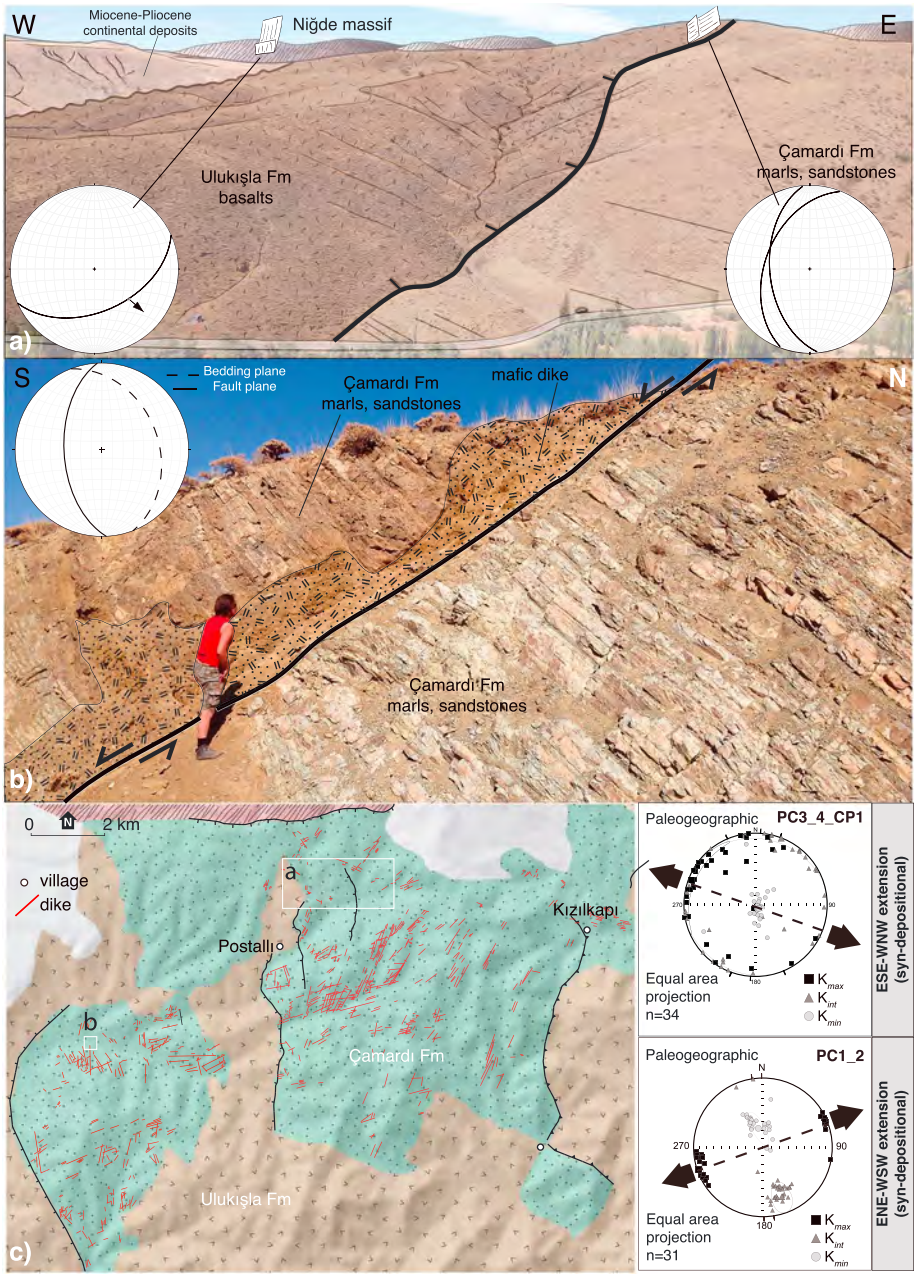

Figure 7. Interpreted field photographs of representative outcrops at the northern basin margin along the road between Postallı and Kızılkapı villages. (a) The contact with the Niğde massif is marked by a top SE fault, a series of west dipping large-offset listric normal faults cuts SE-ward dipping Paleocene turbidites and volcanic rocks. (b) Mafic dike swarms intrude into fault surfaces within the sediments of the Çamardı Formation. AMS plots (inset), located at, or close to photo locations within the Çamardı Formation show WNW-SSE to WSW-ENE extension directions. (c) Map view of dike swarms with roughly E-W and roughly N-S orientation intruded into normal faults in the sediments of the Çamardı Formation.

lineations at the first group (13 sites) to have formed under compressive tectonics, whereas the magnetic lineations of the second group (12 sites) to have formed in an extensional tectonic regime (Figure 5).

5. Structure of the Ulukışla Basin

The sedimentary formations of the Ulukışla region display multiple deformation features that reflect a polyphase tectonic evolution. We have focused our kinematic analysis on major structures across the basin,

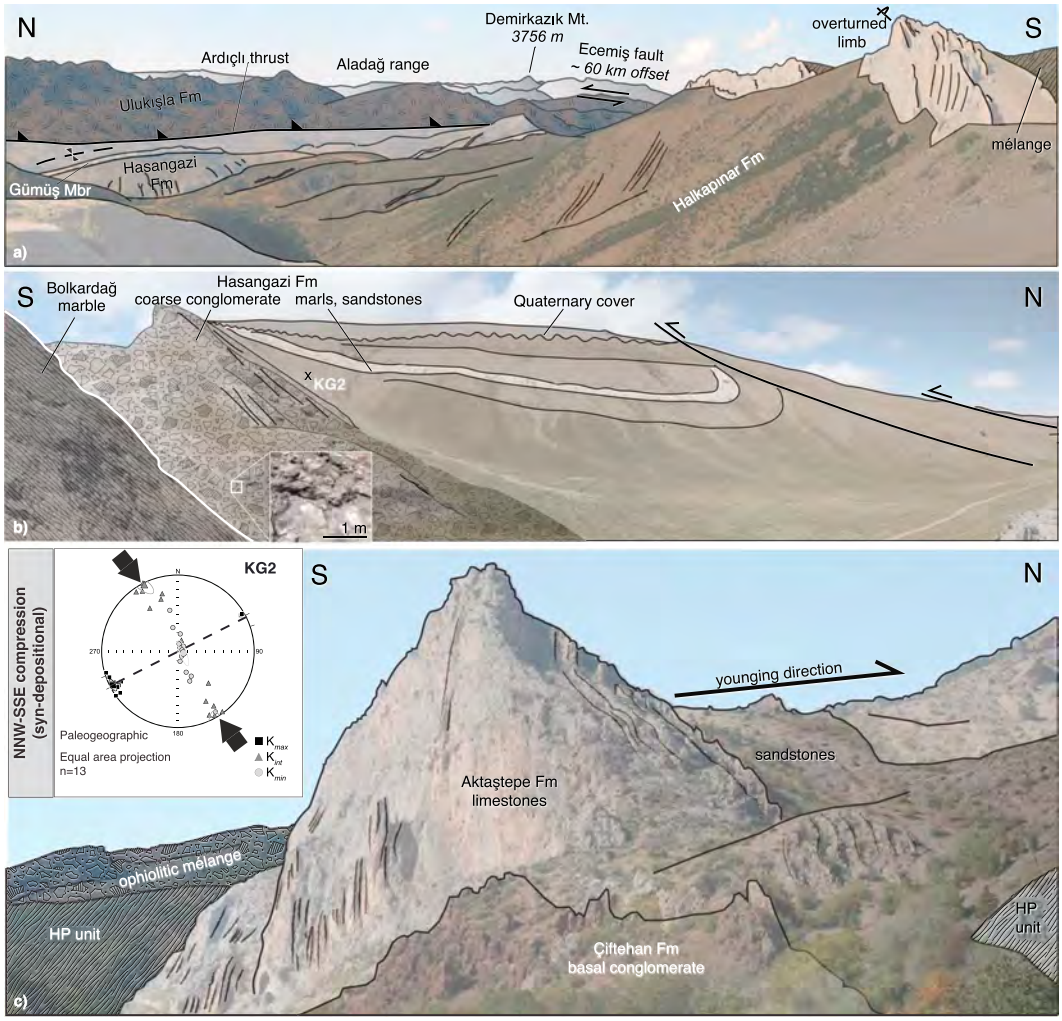

Figure 8. Interpreted field photographs of representative outcrops illustrating Eo-Oligocene and younger shortening at the southern basin margin close to the contact with the Bolkar Mountains, in the northern continuation of the Bolkar anticline. (a and c) Note that basal basin strata are subvertical to overturned. Field of view in top photograph (Figure 8a) is indicated on the geological map in Figure 2. (b) Field relations close to Karagöl (37.412578°, 34.562965°), where the Bolkardağ marbles are unconformably overlain by a coarse conglomerate (reworking ophiolitic and Bolkardağ debris, inset in Figure 8b) and are overlain by Lutetian marls and sandstones that record (synkinematic) outcrop-scale thrusting. The location of AMS sampling site KG2 is indicated in Figure 8b. AMS plot (lower hemisphere equal area) indicative of NNW-SSE compression (inset in Figure 8c). Field view close to Kalkankaya cliff (37.471683°, 34.661271°), where the Aktaştepe Formation is subvertical to overturned, younging to the north (Figure 8c).

such as major normal faults or thrusts, large-scale folds, and strike-slip faults. Our field data include measurements of faults with kinematic shear-sense criteria (such as slickensides, Riedel fractures, drag-folds, and conjugate faults), folds (outcrop scale or regional), and shear zones with cataclastic or semiplastic deformation. Observations on fault and fold relationships provide indications for synkinematic sedimentation (Figures 5a–5d). Successive deformation events mean that the younger deformation can tilt or otherwise rotate older structures. Therefore, structures were restored where necessary to their original position by using tilting indicators, such as rotated conjugate normal faults or the orientation of synkinematic deposits. The latter were identified based on growth strata, wedging against faults, variations in thicknesses, decreasing displacement with stratigraphic level, and structural superposition criteria. The kinematic interpretation has been aided by the construction of regional cross sections (Figures 6a–6c) and the detailed analysis of the key outcrop-scale structures observed in the basin (Figures 7–9). The relative chronology of deformation was derived from this synkinematic sedimentation, combined with fault cross-cutting relationships and superposition of tilting. Previous studies have analyzed the kinematics of the strike-slip structures associated

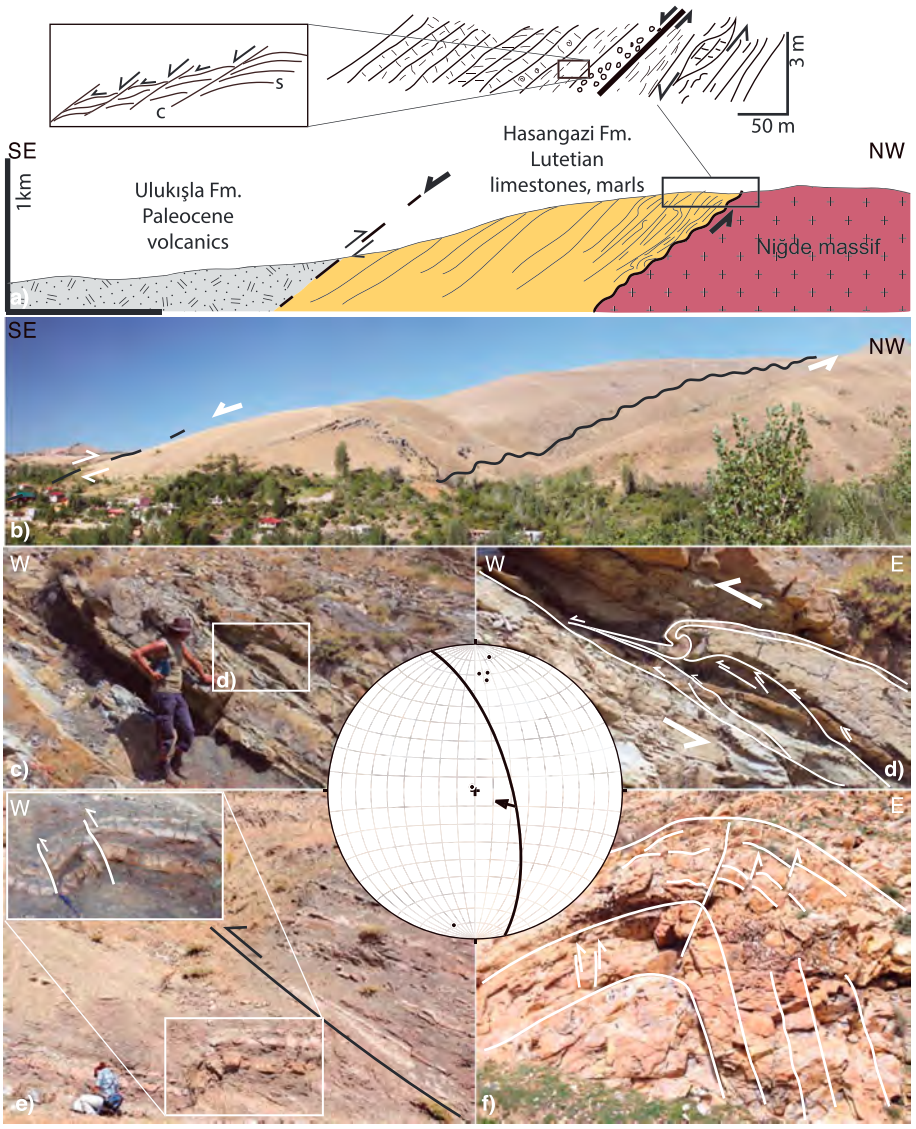

Figure 9. Compressional and transpressional structures observed in the eastern part of the basin, close to the Ecemiş Fault**.** (a and b) The contact between weakly metamorphosed Eocene sediments and the Niğde massif north of Çamardı town. Paleocene volcanic rocks thrusted NW-ward reactivating a top-SSE structure apparent from S-C shear bands in Eocene strata (inset in Figure 9a). Postdepositional transpressional structures indicating E-W shortening along the road section east of Bekçili village (viewing north) within sediments of the Çamardı Formation. These include (c–e) fault propagation folds and (f) N-S trending folds. Photograph locations are indicated on the geological map in Figure 2.

with the sinistral movement of the Ecemiş Fault, which borders the basin to the east [*Jaffey and Robertson*, 2001; *Higgins et al.*, 2015]. Therefore, we have concentrated our analysis elsewhere in the Ulukışla basin to quantify and date older deformation events.

Numerous normal faults have been observed in the field. These are often associated with synkinematic sedimentation and changes in sedimentary facies indicating relative deepening. The normal faults can generally be grouped in two systems (Figures 5a, 5b, and DR2.2), namely, generally E-W striking, and roughly N-S striking. The analysis of the first generation of faults, including back-tilting where necessary, indicates that the older deformation event recorded in the basin is characterized by normal faults with a dominant dip-slip sense of shear indicating a N-S direction of extension (Figure 5a). These normal faults were observed dominantly in the lower part of the stratigraphy affecting the Çiftehan, Halkapınar, and Çamardı Formations (Figure 3) and are particularly well-developed along the Ardıçlı and Üskül road sections in the south of the basin (Figure 5), where the extension is evident from numerous small offset (cm-dm scale) normal faults.

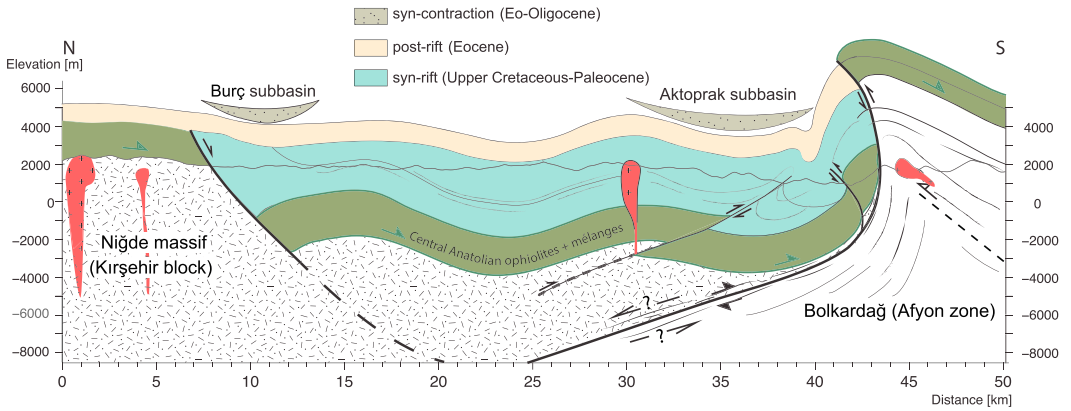

Figure 10. Conceptual composite regional cross section across the Ulukışla basin and its underlying basement units. The roof thrust of ophiolites over basement units is marked by green arrows. The basin infill is subdivided into synrift, postrift, and syncontractional phases. Eocene intrusions are drawn in red.

Many of these faults are syndepositional (e.g., growth faulting) and coeval with changes in facies that are compatible with faulting, such as deepening (Figure DR2.2). Such E-W striking normal faults are less frequent in the northern part of the basin, but where observed (e.g., along the road to Postallı), they are always associated with synkinematic deposition in the Çamardı Formation.

The second, younger normal fault system strikes ~NNE-SSW. Fault analysis, after back-tilting where necessary, indicates a combination of dip-slip and oblique-slip deformation along listric faults with a top-to-the west sense of shear. Normal and oblique-slip normal faults consistent with E-W extension are also found as growth faults in the Çamardı Formation. ~N-S striking normal faults were mapped only in the northern part of the basin (Figures 5, 6c, and 7a) along the road between Kızılkapı and Postallı villages. Typical field examples (Figure 7) show the truncation of the east dipping Çamardı Formation and the volcanic rocks at the base of the Ulukışla Formation along N-S striking, west dipping normal faults with offsets on the order of several hundred meters and hanging wall block rotations along listric normal faults. Mapping the prekinematic and synkinematic sediments in these east dipping strata has allowed a surface to depth projection of the main décollement level at around −1 km above sea level depth (Figure 6c). Normal faults are frequently intruded by mafic dikes (Figure 7b), using fault planes as pathways for magma ascent. Using satellite imagery, we mapped the dike orientations (Figure 7c), which we field-checked in places. These dike swarms interestingly follow N-S and E-W trends. Upward in the stratigraphy, the upper part of the volcanic rocks of the Ulukışla Formation is not displaced by these faults and therefore postdates the extensional events (see section 3.2).

Extensional deformation was followed by contraction, locally associated with transpressional to strike-slip deformation. Outcrop- and regional-scale E-W striking folds and thrust faults (Figures 2, 5, 6a, 6b, and 8) deformed the central and southern parts of the basin. Thrusts are E-W striking, except close to the Ecemiş fault, where they are NE-SW striking, and associated with oblique to strike-slip sense of shear. The transition from thrusting to transpressional deformation in the vicinity of the Ecemiş fault takes place gradually with the change in strike. The wavelength of folds is larger toward the north and west, while they become narrower and higher in amplitude eastward. We illustrate the main large-scale folding and thrusting along two NNW-SSE trending structural profiles (Figures 6a and 6b).

Near the southern margin of the basin, a large-scale, north verging asymmetric fold deforms basement units of the Taurides, including the Bolkardağ metamorphic rocks and the overlying ophiolitic mélange and ophiolites (e.g., Kızıltepe and Alihoca ophiolites), as well as the stratigraphy up to and including the Aktoprak Formation. The fold (hereafter referred to as the Bolkar fold) has a spectacular subvertical to overturned limb that dominates the topography in the southern part of the basin (Figures 8a, 8c, and 10). The amount of horizontal shortening of the Bolkar fold is estimated from the height of its vertical limb in profile B-B′ of Figure 6b at ~4 km.

The northern flank of the Bolkar fold is affected by several thrusts with northward vergence and locally, fewer lower offset ones with southward vergence (Figures 6a and 6b). These faults truncate and tilt all

preexisting extensional structures. The overall intensity of folding and thrusting decreases along-strike toward the west, while thrusts and folds with horizontal hinges are gradually replaced toward the Ecemiş Fault in the east by oblique reverse and transpressive faults associated with folds with high plunges (Figure 5). These observations show clearly that at least part of the displacement of the NNE-SSW oriented Ecemiş Fault is transferred to contraction along the E-W oriented Bolkar structure. A large top-to-the-north thrust, emplacing the Bolkar mountains over the sediments of the Ulukışla basin, has been interpreted in previous studies [*Blumenthal*, 1956; *Demirtasli et al*., 1984]. Although many relatively small offset thrusts affect this contact, no evidence of such a large thrust was observed. The geometry of the Bolkar fold indeed requires accommodation by a thrust in its core, but if such a structure exists, it is likely still buried at depth. This interpretation is in agreement with the smaller displacement thrusts observed in the core of the northern adjacent syncline. One of these thrusts emplaced the succession of sheeted dikes and basalts observed in the upper part of the Alihoca ophiolite over the hemipelagic limestones observed near the base of the Ulukışla stratigraphy.

An interesting structure, showing top-to-the-south thrusting associated with a synkinematic Eocene sequence onlapping onto the Bolkar mountains, was observed close to Karagöl (Figures 6b and 8b). In more detail (Figure 8b), this structure shows an angular unconformity within the Eocene sequence that reflects the formation of a slope by tilting during Eocene shortening. The sequence is transgressive, passing from a proximal conglomerate (likely alluvial) reworking ophiolitic debris (inset Figure 8b), Bolkar marbles, and calcschists to the deposition of (shallow) marine mudstones and sandstones of Lutetian age upward in the stratigraphy (BS11 in the supporting information). The synkinematic wedge and the basal conglomerates are drag-folded by few south vergent thrusts.

The largest structure observed within the basin is the south vergent Ardıçlı thrust that emplaces the Çiftehan Formation over the Ulukışla volcanic rocks with a displacement of a few hundred meters to maximum 1 km (Figures 6a and 6b). This thrust is associated with large-scale drag-folding of its footwall, where a series of smaller displacement thrusts verging both northward and southward were observed (Figures 6a and 6b). The hanging wall of the Ardıçlı thrust is deformed in several open, E-W striking folds affecting the Hasangazi and Bolbeztepe Formations.

Another interesting feature is observed in the southwestern part of the basin. There, a broad zone of ophiolitic mélange is thrusted northward and southward over the Eocene Hasangazi strata that have subvertical bedding planes (Figures 6b and 8a). In addition, within this mélange, abundant nummulitic limestone blocks of the Hasangazi Formation can be found. The overall deformation is likely a décollement fold in the rheologically weak mélange that is associated with a series of "extruded" pop-up structures in the more competent and stratigraphically overlying limestone units (Figure 6b).

In the eastern part of the basin, close to the SE margin of the Niğde massif near Çamardı, numerous structures indicate ~E-W to NW-SE shortening in a zone close to the Ecemiş fault (Figures 2 and 9). These are observed often by N-S trending folds in the Çamardı Formation and west vergent thrusting, such as fault propagation folds east of Bekçili village (Figures 9c–9f). This observation is in agreement with previous studies, which have shown that the weakly metamorphosed Eocene sediments of the Hasangazi (or Evliyatepe [*Göncüoglu et al*., 1991]) Formation unconformably deposited over the Niğde basement, contain tight, asymmetric folds with (north) west vergence [*Umhoefer et al*., 2007; *Idleman et al*., 2014]. Furthermore, we observed that the volcanic rocks of the Ulukışla Formation are thrusted NW-ward over the stratigraphically higher Hasangazi Formation, inverting a former top-SSE structure (Figure 9a). This relationship is marked by numerous brittle S-C shear-bands affecting the Hasangazi mudstones and clastic rocks that stratigraphically overlie the Niğde basement (Figure 9a), suggesting that shearing accommodated the exhumation of the Niğde massif most likely by extensional deformation, as previously inferred [*Umhoefer et al*., 2007; *Gautier et al*., 2008], and was followed by thrusting of the Ulukışla Formation.

In the northern part of the basin, a south dipping high-angle normal fault with abundant striations and local fault brecciations was observed near the southern boundary of the Niğde massif (Figures 5, 6, and 7a). This is an isolated E-W striking dip-slip normal fault that roughly coincides with the previously inferred detachment [*Whitney and Dilek*, 1997], later interpreted as a late stage (Neogene) normal fault [*Gautier et al*., 2002, 2008]. Our data are in agreement with the latter interpretation, as the normal fault coincides with the strain pattern obtained from a Miocene site that is compatible with N-S extension (site CP2;

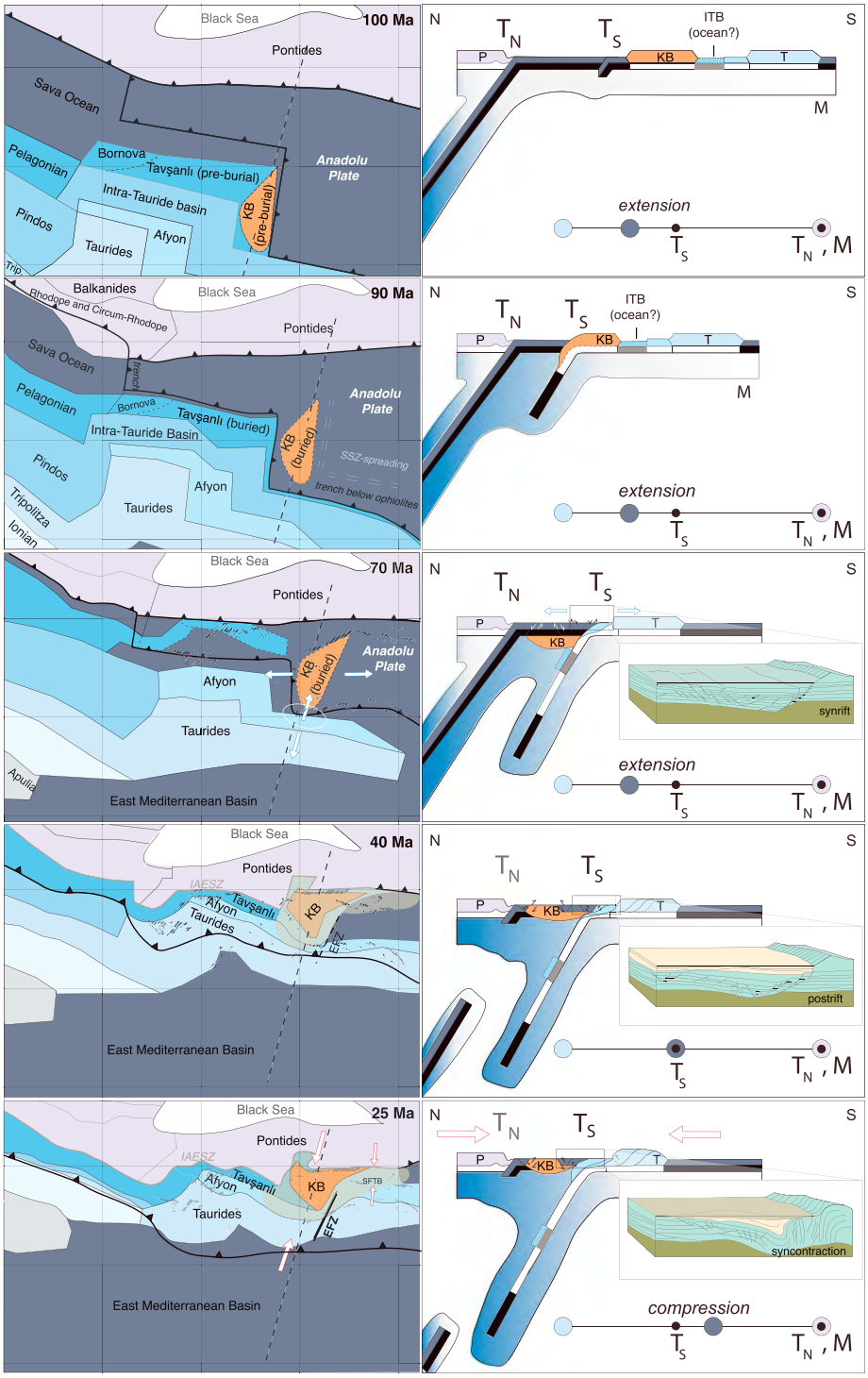

Figure 11. (left column) Plate kinematic evolution of the Central and Eastern Anatolian region and the Anadolu Plate through time illustrated in map view (based on the reconstruction of *van Hinsbergen et al.* [2016] in Central Anatolia and on *van Hinsbergen and Schmid* [2012] for Western Turkey and Greece), and (right column) lithospheric-scale cross sections (location indicated by dashed black line), basin-scale cross sections illustrating the different stages of basin development, accompanying relative motion paths. The location of the Ulukışla basin is marked by the white circle at 70 Ma. The semi-transparent light brown area represents the location of the Central Anatolian basins. Abbreviations used are as follows: KB = Kırşehir block, P = Pontides, T = Taurides, T_N = northern trench, T_S = southern trench, M = mantle, IAESZ = Izmir-Ankara-Erzincan Suture Zone, ITB = Intra-Tauride basin, SFTB = Sivas fold-thrust belt, EFZ = Ecemiş Fault Zone. The black triangles indicate the active subduction zone, the gray line indicates the suture, and the dark blue hatched areas indicate the Anatolian ophiolites.

Figure 5 and the supporting information). The relative importance of this late-stage Miocene deformation is relatively poorly constrained in the basin outside this individual structure and therefore difficult to interpret in the overall tectonic evolution. The last type of deformation observed in the basin is represented by postdepositional strike-slip faults with NNE-SSW or NW-SE strike, which are often transtensional or transpressional (Figure 5d).

6. Tectonic Interpretation of the Ulukışla Basin

Our overall field observations combined with biostratigraphic data and AMS fabric analysis show a multiphase tectonic evolution of the Ulukışla basin that is almost continuous and partly coeval with the evolution of its underlying basement units (Figures 10 and 11). In the upper part of this basement, the age of the oceanic crust of the Alihoca ophiolite is ~92 Ma, comparable with the $^{40}Ar/^{39}Ar$ age obtained from hornblende in a mafic dike (90.8 ± 0.8 Ma [*Dilek et al*., 1999]). The suprasubduction zone geochemistry of this ophiolite [e.g., *Yaliniz et al*., 1996, 2000a; *Yaliniz and Göncüoglu*, 1998; *Dilek et al*., 1999; *Parlak et al*., 2000; *Yaliniz*, 2008] suggests that its formation shortly postdated subduction initiation in the vicinity of an oceanic spreading center [e.g., *Dilek et al*., 1999; *van Hinsbergen et al*., 2016].

The deepwater sediments of the "first sedimentary package" of the Çiftehan Formation observed near the southern margin of the basin were deposited during Campanian times and were subsequently uplifted together with the underlying ophiolites and their mélange above an accretionary wedge of Tauride-derived rocks during Campanian-Maastrichtian times. This continental underthrusting below the ophiolites is widely referred to as the ophiolite's obduction, which was previously dated as Campanian-Maastrichtian, based on the age of the limestone blocks in the ophiolitic mélange observed in the southern part of the basin [*Robertson et al*., 2009]. The uplift of the ophiolites and the overlying first sedimentary package of the Çiftehan Formation occurred prior to ~65 Ma as shown by $^{40}Ar/^{39}Ar$ cooling ages in the underlying Bolkardağ unit [*Pourteau et al*., 2013].

Coeval with the uplift of the ophiolite and its underlying mélange during continental underthrusting, the onset of Ulukışla basin sedimentation was recorded during Campanian-Maastrichtian times in its central parts. This is marked by the deposition of the continental conglomerates and the subsequent transgression that migrates in space and time. Observations and biostratigraphic dating show that deposition started over the basal unconformity during the Campanian in the central part of the basin, the transgression extending the basin toward its present-day margins during Maastrichtian times. The onset of basin deposition took place during the N-S extension, as demonstrated by numerous faults with synkinematic deposition observed in the basal Campanian-Maastrichtian sequence.

These overall observations demonstrate that the onset of Ulukışla basin deposition took place in a N-S extensional setting during the N-S oriented Campanian-Maastrichtian collisional emplacement of the Central Anatolian ophiolites. This deposition gradually covered the Niğde massif and the ophiolites in its hanging wall, the Alihoca ophiolite and mélange, and ultimately, the margin of the Tauride nappe stack. Such setting demonstrates that the Ulukışla basin was initiated as a Campanian-Maastrichtian fore-arc basin.

The initial N-S oriented extension was associated with the exhumation and erosion of the metamorphic rocks of the Bolkardağ unit, documented by their deposition in the coarse conglomerates at the base of the Halkapınar Formation in the southern part of the basin. These conglomerates also contain abundant nonmetamorphic carbonates, suggesting that at least part of the Tauride fold-thrust belt was already uplifted and available for erosion [see also *Clark and Robertson*, 2002, 2005]. Such a genetic relationship infers the presence of a large-scale extensional detachment separating the Ulukışla basin in its hanging wall from the metamorphic unit in the footwall, although the presence of such a structure requires further analysis in the latter unit. Note that there is no direct contact between the Paleocene-lower Eocene Halkapınar Formation and the Bolkardağ metamorphic rocks. These units are always separated by the ophiolites and/or their associated mélange.

The initial N-S orientation of extension changed subsequently to E-W during Paleocene times, as observed in the northern part of the basin by large-displacement west dipping listric normal faults (Figures 7a and 7b). AMS data confirm that E-W extension was active during the deposition of the Çamardı Formation (Figures 5 and 7b, and the supporting information). The base of the Ulukışla Formation in the northern part

of the basin, including a lava that we dated at ~60 Ma, is displaced by normal faults (Figure 7a). The top of the formation, close to our 56 Ma age (Figure 3), is not affected by this deformation. E-W extension thus ceased between 60 and 56 Ma.

In the southern part of the basin, the strain recorded by the basal stratigraphy was largely overprinted by intense post-Eocene shortening, resulting in the observed triaxial AMS fabrics (Figure DR2.1). Extensional patterns are still preserved, especially in the northern AMS sites, which confirm the E-W extension documented in our kinematic analysis.

The Late Cretaceous-Paleocene extension was followed by contraction. The onset of contraction started during the deposition of the Lutetian Hasangazi Formation, as evidenced by the gradual onlapping sequence observed at Karagöl and the AMS site (KG2) derived from the marls of the same sequence (Figure 8b). Contraction led to formation of the major north verging asymmetric Bolkar fold, and associated subordinate thrusting in the adjacent syncline (Figures 6a and 6b). Although the topographic expression of the shortening is spectacular, the amount of horizontal shortening was only ~4 km (Figures 6a, 6b, and 8). Our AMS data suggest that the deposition of the redbeds of the Aktoprak Formation, in the late Oligocene [*Blumenthal*, 1956; *Meijers et al*., 2016], occurred during continued Bolkar folding, consistent with the molasse-type sedimentary facies. Apatite fission track ages of 23–16 Ma from the Horoz granite [*Karaoglan*, 2016] exposed in the vertical limb of the Bolkar anticline indicate that the exhumation continued during Miocene times, following the initial onset of contraction associated with Bolkar folding and uplift. The Bolkar anticline is restricted to the area south of the Ulukışla basin, bordered in the east by the Ecemiş fault. The intensity and amount of uplift of the Bolkar anticline disappears westward. The Mut basin, which overlies the central Tauride fold-thrust belt, contains upper Oligocene lacustrine deposits and lower to upper Miocene marine deposits [*Bassant et al*., 2005]. It clearly remained at low elevations until at least the late Miocene [*Radeff et al*., 2012; *Schildgen et al*., 2012]. The Mut basin, as well as the Adana basin, underwent major late Miocene and younger uplift raising it to ~2 km, considered to reflect the uplift during the rise of the Central Anatolian Plateau [*Clark and Robertson*, 2005; *Jaffey and Robertson*, 2005; *Schildgen et al*., 2012; *Fernández-Blanco et al*., 2013; *Meijers et al*., 2016] Therefore, the Bolkar Mountains, exposing metamorphosed rocks in their core at elevations reaching close to 3500 m, likely underwent a two-stage uplift history: the first one related to Bolkar folding up to the late Oligocene-early Miocene likely produced the elevation difference with the Mut basin of ~1500 m, and the second one created by the latest Miocene and younger regional uplift that brought the Mut basin to 2 km elevation.

The ~W-E to NW-SE shortening illustrated SE of Niğde (Figures 9f–9f) demonstrates that there was a component of contraction associated with motion along the Ecemiş Fault. In combination with its demonstrated ~60 km left-lateral displacement, the Ecemiş Fault must have been a transpressional structure leading to reburial of the Niğde basement, as previously inferred [*Fayon et al*., 2001; *Whitney et al*., 2003; *Umhoefer et al*., 2007; *Idleman et al*., 2014]. The thrusting of the Ulukışla Formation over Lutetian limestones of the Hasangazi Formation shows that this shortening occurred after the Lutetian in the northern part of the basin. In addition, the stratigraphy of the Ecemiş corridor, interpreted to be syndepositional with Ecemiş displacement [*Jaffey and Robertson*, 2001, 2005] was interpreted as Eo-Oligocene age, i.e., roughly time-equivalent with the sediments of the Aktoprak syncline. Hence, we interpret the Ecemiş Fault zone to be at least partly coeval and kinematically related to the N-S shortening forming the Bolkar fold and related folds and thrusts in the basin.

The re-exhumation of the Niğde massif after its Oligocene reburial to several kilometers depth was estimated to have occurred in the Miocene, based on apatite fission track ages of ~10 Ma [*Fayon et al*., 2001]. This exhumation was clearly extensional, as shown by the top-to-the-SE S-C fabrics developed in the Lutetian sediments of the Hasangazi Formation overlying the SE Niğde massif (Figure 9a). To explain this extension, *Whitney et al*. [2007] and *Idleman et al*. [2014] suggested that in Miocene time, the sense of shear along the Ecemiş Fault became right-lateral, leading to a transtensional reactivation of former transpressional faults. Lower Miocene marine sediments in the Adana basin to the south of the Ecemiş corridor, however, are not significantly displaced by the Ecemiş Fault (Figure 1). If right-lateral strike-slip of sufficient magnitude to exhume the Niğde massif (i.e., several kilometers) had occurred, it should have been accommodated in a compressional horsetail structure within the Aladağ Mountains or an extensional horsetail within the Ulukışla basin. No evidence exists for either such structure. We find it therefore not likely that the Miocene extensional exhumation was related to a reversal of Ecemiş Fault motion. It was recently shown that Quaternary faulting along the Ecemiş Fault accommodated E-W extensional motion [*Higgins et al*., 2015;

Sarıkaya et al., 2015; *Yıldırım et al*., 2016], making the fault dominantly a normal fault in recent time. E-W extensional faulting has also been documented in Miocene time in the eastern Tuzgölü basin [*Fernández-Blanco et al*., 2013; *Özsayin et al*., 2013], as well as in the basins along the eastern margin of the Western Taurides [*Koç et al*., 2014, 2015]. We therefore suggest that the reactivation of the Niğde structure is more likely explained by modest, regionally persistent E-W extension. Such extension may explain why the formerly transpressional Ecemiş Fault that must have juxtaposed the Aladağ mountains against the E-W shortened Ulukışla basin sediments is presently separated from these by a several kilometer-wide valley parallel to the fault.

7. Discussion

7.1. Implications for Central Anatolian Tectonics

We will now discuss how the tectonic history of the Ulukışla region fits with and constrains the tectonic history of Central Anatolia. To this end, we compare the sedimentation and surface deformation history of the Ulukışla basin with the relative motions of the underlying basement units of the Bolkardağ (Afyon zone) and the Niğde massif.

Our detailed kinematic data confirm and build upon an important extensional phase in the Ulukışla region that was previously inferred based on facies observations, geochemistry of volcanic rocks, and subsidence curves [*Clark and Robertson*, 2002, 2005]. Based on fault kinematic data, we have shown that there are two systems of normal faults (N-S and E-W). E-W extension, which we showed deformed the northern part of the Ulukışla basin in latest Cretaceous-Paleocene times, is widespread to the north of the study area. There, E-W extensional detachments and shear zones were active during the exhumation of the high-grade metamorphic rocks of the Kırşehir block [*Gautier et al*., 2002, 2008; *Isik et al*., 2008; *Isik*, 2009; *Lefebvre et al*., 2011, 2015]. Cooling histories of the Kırşehir block suggest that extensional exhumation was active from 75 to at least ~65 Ma [e.g., *Whitney et al*., 2003, 2007; *Umhoefer et al*., 2007; *Gautier et al*., 2008; *Idleman et al*., 2014]. In the Ayhan-Büyükkışla supradetachment basin, extension prevails until at least after 72 Ma [*Advokaat et al*., 2014], and ceased prior to the Lutetian. Our study suggests that E-W extension in Central Anatolia continued until 60–56 Ma. We interpret this age to reflect the end of the regional extension in Central Anatolia. A regional marine transgression subsequently led to widespread deposition of Lutetian limestones on the Kırşehir block [*Göncüoglu et al*., 1991, 1992; *Köksal and Göncüoglu*, 1997; *Gülyüz et al*., 2013; *Advokaat et al*., 2014]. E-W extension has progressively migrated farther west, where it has been active into the Miocene [*Fernández–Blanco et al*., 2013; *Özsayin et al*., 2013; *Koç et al*., 2014, 2015].

Previously, it has been suggested that the Ulukışla basin also represented a supradetachment basin of the Niğde massif [e.g., *Whitney and Dilek*, 1997]. In the absence of a detachment surfacing to the east or west of the basin, this is hard to judge, but we suspect that the west dipping listric normal faults may indeed root into an extensional décollement at depth. In any case, the amount of E-W extension in the Niğde massif was significantly larger than in the northern Ulukışla basin, and no evidence for E-W extension was found in the southern part of the basin.

During E-W extension, N-S extension was also active in the Ulukışla basin. Furthermore, dikes intruding N-S trending normal faults (Figure 7c) have been observed in numerous locations within the Çamardı Formation in the northern part of the basin, suggesting a strong spatial correlation between the normal fault systems. The orientation of dikes perpendicular to the two extension directions, observed in the northern part of the Ulukışla basin, is consistent with our inferred two-stage extension. This demonstrates that the volcanism was associated with the overall extension.

With the currently available evidence, it is hard to judge the overall importance of this extension. It may reflect the stress state inflicted by the northward dipping subduction zone, which must have existed below the Taurides to the south of the basin. On the other hand, normal faulting in overriding plates close to trenches is common in times of subduction erosion [e.g., *von Huene and Scholl*, 1991; *von Huene et al*., 2004; *Stern*, 2011]. If extension is of local scale, it may be well possible that normal faulting is mainly controlled by basal tectonic erosion and subsequent subsidence of the overriding lithosphere. However, if this were the case, we would expect trenchward dipping normal faults [*Clift and Vannucchi*, 2004]. Furthermore, the Late Cretaceous to Paleocene history of the Taurides appears to be dominated by accretion rather than subduction erosion [*Monod*, 1977; *Gutnic et al*., 1979; *Demirtasli et al*., 1984; *Özgül*, 1984]. We also

note that during Paleocene times, the Bolkardağ HP-LT metamorphic rocks were exhumed to the surface, although the structures that accommodated this motion have not been documented yet. In any case, the presence of HP rocks at the surface suggests that there was space at the subduction contact, allowing for backflow of material from depth. If the subduction contact was in extension on a larger scale (i.e., regional), the extension observed in the our study area must have been driven by overriding plate advance or slab roll-back [*Uyeda and Kanamori*, 1979]. Because we do not have constraints on the scale at which this extension was active, we cannot clearly discern between the two possibilities. It is possible that the small-scale normal faults in the basal stratigraphy are part of a generation of trench-parallel faults with larger offsets.

N-S directed shortening is distributed across Central Anatolia, and the onset of this shortening becomes younger from north to south. It is latest Cretaceous to Paleocene in the Central Pontides [*Meijers et al*., 2010; *Espurt et al*., 2014], Paleocene in the Çankırı basin [*Kaymakci et al*., 2009], late Eocene in the Çiçekdağı basin [*Gülyüz et al*., 2013], late Eo-Oligocene in the Ayhan-Büyükkışla basin [*Advokaat et al*., 2014], and probably late Eocene-Oligocene in the Ulukışla basin (this paper). N-S shortening of Central Anatolia probably stopped in early Miocene time [*Kaymakci et al*., 2009]. This phase of deformation was also synchronous with and likely accommodated regional block rotations in the Kırşehir block [*Lefebvre et al*., 2013]. The Ecemiş Fault with its $>$60 km displacement disrupts the connection between the Ulukışla and Sivas basins (Figure 1). The area to the east of this fault, which aligns with and is probably controlled by the eastern margin of the Niğde massif, must have accommodated $>$60 km more N-S Eo-Oligocene convergence than Central Anatolia. The Ecemiş Fault thus transferred shortening in the Ulukışla basin and to the south of the Taurides to the Sivas region in eastern Turkey. This lead to the structural growth of the Sivas fold-thrust belt since the latest Eocene time, which played a major role in marine basin isolation, disconnection from the Ulukışla basin, and a regionally important transition to continental conditions with evaporite deposition starting in early Oligocene times [*Ribes et al*., 2015; *Kergaravat et al*., 2016; *Pichat et al*., 2016].

7.2. Paleo-plate and Trench Kinematics

Numerical models [*Čížková and Bina*, 2015; *Jagoutz et al*., 2015] have explored the dynamics of interacting slabs and the resulting kinematics of double subduction zones with the same polarity. Double slabs create complex dynamic pressure and mantle flow fields, and an additional slab pull force originating from the frontal slab is transmitted across the subduction zone interface of the rear one. This increases the dip angle of the rear slab due to the opposite torques of the pressure cells. Similarly, *Čížková and Bina* [2015] conclude that in a three-plate system, slab-pull exerted by the central plate may enhance advance of the rear trench.

While on modern-day Earth such ongoing double-subduction-induced trench advance may be unique to the eastern boundary of the Philippine Sea Plate, similar double-subduction geometries have been postulated to drive the ultrarapid northward advance of India in the Paleogene prior to collision with Eurasia [*Jagoutz et al*., 2015], and more generally during prior intraoceanic subduction of regions of the Neotethys [*Agard et al*., 2011; *van Hinsbergen et al*., 2015; *Van Hunen and Miller*, 2015]. In this section, we develop a concept on how we may use the geological observations from Central Anatolia to constrain the kinematic evolution of the now largely subducted plate of the Neotethys of which the Alihoca ophiolite is a relict. Thereby, we introduce a plate kinematic scenario for the Neotethyan Ocean that covered the paleogeographic realm that existed between the Pontides and the Taurides. Our analysis shows that the oceanic crust that floored the Neotethyan ocean in Turkey must have been part of at least two tectonic plates: a southern portion was part of the African Plate, together with the Anatolide-Taurides, whereas a northern portion was, at least since the initiation of subduction at ~100–95 Ma, part of a separate tectonic plate, which we term "Anadolu Plate" (after the Turkish word for Anatolia). The paleo-plate configuration is illustrated in the conceptual N-S cross sections showing three plates bounded by two subduction zones (Figure 11).

An original northern plate contains the Pontides (Eurasia), thereby ignoring extensional tectonics in the Black Sea [e.g., *Nikishin et al*., 2015; *Sosson et al*., 2015] for simplicity. The southern one contains the Taurides—at least at the beginning of subduction in the Late Cretaceous—and is indicated as Africa. This simplification ignores any subduction that may have occurred between the Taurides and Africa [e.g., *Robertson*, 2000; *Çetinkaplan et al*., 2016]. The Anadolu Plate in the middle is oceanic in nature, and formed the overriding plate relative to the Taurides/Africa, and the downgoing plate relative to the Pontides/Eurasia. Our study area and most of Central Anatolia reflect the remains of this central plate. As a final simplification, the Pontides and the

trench bounding the Pontides to the south are assumed to be stationary relative to the mantle. This is consistent with mantle reference frames [*Doubrovine et al*., 2012] that do not show significant northward or southward motion of Eurasia at the location of the Central Pontides in the time interval of our study. The results and interpretations presented above are defined in terms of relative motions of these three plates and trenches.

We illustrate the plate kinematic history as map-view configurations through time, building on *van Hinsbergen et al*. [2016], and as a series of N-S oriented lithospheric and idealized basin-scale cross sections (Figure 11). Below each cross section, we show a velocity line [*Cox and Hart*, 1986] that portrays the relative motions between the African, Eurasian, and Anadolu Plates, as well as the intervening trenches (Figure 11). The discussion is focused on the N-S cross sections and ignores the effects of the N-S striking, eastward dipping, oblique subduction segment (Kırşehir segment) that must have existed to the west of the Kırşehir block, connecting the north dipping subduction segment south of the Ulukışla basin with the one in northwestern Turkey [*Advokaat et al*., 2014; *Gürer et al*., 2014; *van Hinsbergen et al*., 2016].

The situation of double northward subduction initiated ~100–95 Ma close to a former spreading ridge between Anadolu and Africa. From this time onward, the Taurides (Africa) converged with Anadolu, and Anadolu converged with the Pontides (Eurasia). At ~92 Ma, the oceanic Anadolu Plate was spreading above the slab subducting at trench T_S (which essentially means that Anadolu consisted of at least two plates at that time) forming the future Alihoca ophiolite. At this stage, we do not know whether the spreading of the Alihoca ophiolite was N-S directed, or E-W, such as in the Sarıkaraman ophiolite to the north [*van Hinsbergen et al*., 2016]. If we, for the sake of the development of our conceptual model, assume that spreading was N-S, this would require that the Anadolu Plate moved northward relative to trench T_S. The Alihoca ophiolite and overlying Ulukışla basin uplifted to sea level in Campanian-Maastrichtian time, which likely reflects accretion of the Tauride nappes below the ophiolite. We have no data on whether the Anadolu Plate was in extension or compression during this time. In Maastrichtian to Paleocene time, we found evidence for N-S extension recorded by the basal sedimentary formations of the basin between ~70 and 56 Ma (arrows in Figure 11), which we portray as once again (slow) northward motion of Anadolu relative to T_S.

From ~56 Ma until shortly before the Lutetian (49–41 Ma), the Ulukışla region experienced tectonic quiescence, suggesting that no relative motion occurred between trench T_S and Anadolu. To the north, the Kırşehir block that accreted to the Anadolu Plate in the Late Cretaceous and started colliding with the Pontides at ~65 Ma, led to shortening in the overriding plate of T_N in Paleocene time [*Kaymakci et al*., 2009; *Meijers et al*., 2010; *Espurt et al*., 2014]. T_N in this time interval hence advanced relative to Eurasia. The collision eventually must have led to slab-break-off at trench T_N at an uncertain time. An age of ~50 Ma was proposed based on widespread volcanism of that age in the T_N suture zone [*Keskin*, 2007]. Slab break-off and cessation of subduction at T_N meant the end of the Anadolu Plate as a separate plate, which then became part of Eurasia (or of the Africa-Eurasia plate boundary zone).

Between ~40 and ~25 Ma, the Anadolu Plate experienced N-S shortening (Figure 11). Restoring the rotations recovered from the Kırşehir block [*Lefebvre et al*., 2013] suggests as much as 250 km N-S contraction in this time period, consistent with folding and thrusting. T_S therefore advanced relative to the Anadolu Plate and Eurasia (Figure 11, arrows). Finally, since 20 Ma, the former Anadolu Plate did not experience major N-S extension or compression. Trench T_S thus became more or less stationary relative to Eurasia.

The conceptual model illustrated in Figure 11 may allow bringing the complex tectonic evolution of Central Anatolia back to a relatively simple plate kinematic scenario, in which the relative motion of the Anadolu Plate relative to Africa and Eurasia gradually decreased. Before ~100–95 Ma, the Anadolu Plate moved faster to the north than Africa, which was accommodated at a spreading ridge between these plates. Since 100–95 Ma, Africa's northward motion was faster than Anadolu's, but Anadolu moved northward relative to the intervening trench T_S and extended. From ~60 to 40 Ma, northward motion of Anadolu and trench T_S was equal, and both advanced relative to Eurasia. From 40 to 20 Ma, Anadolu's northward motion relative to Eurasia had ceased, but northward trench advance of trench T_S continued, with contraction of the Anadolu Plate as a result. After 20 Ma, the location of trench T_S became stationary relative to Eurasia.

The ongoing advance of trench T_S relative to Eurasia between 40 and 20 Ma is peculiar, because it cannot be explained by a northward pull of the Anadolu Plate at the trench T_N below the Pontides, which had

terminated by that time. The ongoing advance of the trench T_S into Central Anatolia expressed by regional N-S shortening may be the subject of a future study on the geodynamics driving Anatolian deformation. We note that the N-S profiles of Figure 11 are simplified and do not take into account the significant E-W extension that affected Central Anatolia in the Cretaceous to Cenozoic. The 4-D kinematic evolution of Anatolia's complex deformation history will be the subject of future papers, using the concept to translate geologically recorded deformation as guide for plate kinematic evolution that we provided here.

8. Conclusions

In this paper, we developed a conceptual model that used geologically recorded deformation in the overriding plate close to the trench as guide to reconstructing the kinematic evolution of a subducted plate that was entirely surrounded by trenches. To this end, we provide new kinematic, stratigraphic, and geochronological data from the Ulukışla basin that overlies relics of the once present oceanic Anadolu Plate. Subduction below this plate initiated ~100–95 Ma. Our conclusions can be summarized as follows:

1. Shortly after subduction initiation, the Anadolu Plate experienced spreading in the overriding lithosphere close to the trench, forming the Alihoca ophiolite below the Ulukışla basin, with a new U/Pb gabbro age of 92.38 ± 0.48 Ma.
2. The ophiolite and overlying stratigraphy became uplifted to close to sea level in the Campanian, likely reflecting accretion of Tauride nappes below the Alihoca ophiolite.
3. ~N-S extension in Campanian-Maastrichtian times followed by ~E-W extension in Paleocene times led to the renewed creation of accommodation space occupied by the sediments of the Ulukışla basin.
4. Our geochronological data show that E-W extension, accommodated along major listric normal faults, which are probably related to regional E-W extension to the north of the Ulukışla basin (where it had started prior to ~75 Ma as recorded the Kırşehir block) prevailed until ~60–56 Ma. This regional E-W extension may be related to westward retreat of the N-S trending Kırşehir segment that bounded the Kırşehir block to the west.
5. From ~56 Ma until ~49 Ma, the Ulukışla basin remained tectonically relatively quiet.
6. Between ~49 and 20 Ma, the Ulukışla basin became shortened in a N-S direction, creating the major north-verging Bolkar fold, and subordinate folds and thrusts in the syncline hinge zone that occupies the southern part of the basin.
7. We use the deformation history of the Ulukışla basin to conceptually infer past relative plate and trench motions. The geology of Central Anatolia can be explained by a three-plate system in Cretaceous to Paleogene time: Africa, Eurasia, and a third, intervening oceanic plate separated from these by trenches. We name the oceanic plate system in between the two trenches "Anadolu." We infer that a gradual deceleration of Anadolu relative to Africa created a trench between these plates along a former ridge. This trench advanced northward toward Eurasia. Even after Anadolu-Eurasia convergence had ceased around 50–40 Ma, northward trench advance continued until ~20 Ma, shortening the former Anadolu Plate.
8. Deformation recorded in the geological record of convergent plate boundary zones, and especially in sedimentary basins forming on the leading edge of the overriding oceanic plate, can be used to develop first-order plate kinematic histories of plates that no longer exist.

Acknowledgments

D.G. and D.J.J. vH. acknowledge financial support through ERC Starting Grant 306810 (SINK). D.J.J. vH. acknowledges NWO VIDI grant 864.11.004. Murat Özkaptan, Nuretdin Kaymakçı, and Loes van Unnik-Hoorn are thanked for logistical support, field assistance, and discussion. Ercan Özcan and Demir Altıner are thanked for providing age information on foraminiferal assemblages. D.G. is grateful to Alexis Plunder, Côme Lefebvre, and Maud Meijers for fruitful discussions about the geology of Turkey, and to Marco Maffione for help with the interpretation of AMS results. Mathew Domeier is thanked for valuable suggestions on an early version of the manuscript. Ton Markus (UU Cartography) is thanked for support with map figures. Laura Swinkels and Dirk Simon are thanked for field assistance in 2013 and 2015, respectively. Many thanks to Recep Ince and Zeynep Tantekin of Aladağlar Camping for logistical support and their hospitality. We gratefully acknowledge the Associate Editor Taylor Schildgen, A.H.F. Robertson, and an anonymous reviewer for their useful comments. The data used are listed in tables, figure references, and supporting information.

References

Advokaat, E. L., D. J. J. van Hinsbergen, N. Kaymakci, R. L. M. Vissers, and B. W. H. Hendriks (2014), Late Cretaceous extension and Palaeogene rotation-related contraction in Central Anatolia recorded in the Ayhan-Büyükkışla basin, *Int. Geol. Rev.*, *56*(15), 1813–1836, doi:10.1080/00206814.2014.954279.

Agard, P., J. Omrani, L. Jolivet, H. Whitechurch, B. Vrielynck, W. Spakman, P. Monié, B. Meyer, and R. Wortel (2011), Zagros orogeny: A subduction-dominated process, *Geol. Mag.*, *148*(5–6), 692–725, doi:10.1017/S001675681100046X.

Alan, I., Ş. Şahin, and B. Bakırhan (2011a), Turkish geological map series, Adana N33.

Alan, I., B. Bakırhan, and H. Elibol (2011b), Turkish geological map series, Karaman N32.

Alpaslan, M., D. Boztuğ, R. Frei, A. Temel, and M. A. Kurt (2006), Geochemical and Pb–Sr–Nd isotopic composition of the ultrapotassic volcanic rocks from the extension-related Çamardı-Ulukışla basin, Niğde Province, Central Anatolia, Turkey, *J. Asian Earth Sci.*, *27*(5), 613–627.

Atabey, E., M. C. Göncüoglu, and N. Turhan (1990), Turkish geological map series, Kozan M33 (J19).

Bassant, P., F. S. P. Van Buchem, A. Strasser, and N. Görür (2005), The stratigraphic architecture and evolution of the Burdigalian carbonate-siliciclastic sedimentary systems of the Mut Basin, Turkey, *Sediment. Geol.*, *173*(1), 187–232.

Blumenthal, M. M. (1956), Yüksek Bolkardağın kuzey kenar bölgelerinin ve batı uzantılarının jeolojisi: (Güney Anadolu Torosları), Maden Tetkik ve Arama Enstitüsü.

Borradaile, G. J. (1988), Magnetic susceptibility, petrofabrics and strain, *Tectonophysics*, *156*(1), 1–20.
Borradaile, G. J. (1991), Correlation of strain with anisotropy of magnetic susceptibility (AMS), *Pure Appl. Geophys.*, *135*(1), 15–29.
Boztuğ, D., R. C. Jonckheere, M. Heizler, L. Ratschbacher, Y. Harlavan, and M. Tichomirova (2009), Timing of post-obduction granitoids from intrusion through cooling to exhumation in central Anatolia, Turkey, *Tectonophysics*, *473*(1–2), 223–233, doi:10.1016/j.tecto.2008.05.035.
Boztuğ, D., E. Türksever, M. Heizler, R. C. Jonckheere, and M. Tichomirowa (2009a), 207Pb-206Pb, 40Ar-39Ar and apatite fission-track geothermochronology revealing the emplacement, cooling and exhumation history of the Karaçayir Syenite (N Sivas), East-Central Anatolian, Turkey, *Turkish J. Earth Sci.*, *18*, 109–125.
Boztuğ, D., O. Güney, M. Heizler, R. C. Jonckheere, M. Tichomirowa, and N. Otlu (2009b), 207Pb-206Pb, 40Ar-39Ar and fission-track geothermochronology quantifying cooling and exhumation history of the Kaman-Kırşehir region intrusions, Central Anatolia, Turkey, *Turkish J. Earth Sci.*, *18*, 85–108.
Candan, O., M. Çetinkaplan, R. Oberhänsli, G. Rimmelé, and C. Akal (2005), Alpine high-P/low-T metamorphism of the Afyon Zone and implications for the metamorphic evolution of Western Anatolia, Turkey, *Lithos*, *84*(1–2), 102–124, doi:10.1016/j.lithos.2005.02.005.
Carminati, E., M. Lustrino, and C. Doglioni (2012), Geodynamic evolution of the central and western Mediterranean: Tectonics vs. igneous petrology constraints, *Tectonophysics*, *579*, 173–192.
Çelik, Ö. F., M. Delaloye, and G. Feraud (2006), Precise 40Ar–39Ar ages from the metamorphic sole rocks of the Tauride Belt Ophiolites, southern Turkey: Implications for the rapid cooling history, *Geol. Mag.*, *143*(02), 213, doi:10.1017/S0016756805001524.
Çelik, Ö. F., A. Marzoli, R. Marschik, M. Chiaradia, F. Neubauer, and I. Öz (2011), Early–Middle Jurassic intra-oceanic subduction in the İzmir-Ankara-Erzincan Ocean, Northern Turkey, *Tectonophysics*, *509*(1–2), 120–134, doi:10.1016/j.tecto.2011.06.007.
Çemen, I., M. C. Göncüoglu, and K. Dirik (1999), Structural evolution of the Tuzgölü basin in Central Anatolia, Turkey, *J. Geol.*, *107*(6), 693–706.
Çetinkaplan, M., A. Pourteau, O. Candan, O. E. Koralay, R. Oberhänsli, A. I. Okay, F. Chen, H. Kozlu, and F. Şengün (2016), P–T–t evolution of eclogite/blueschist facies metamorphism in Alanya Massif: Time and space relations with HP event in Bitlis Massif, Turkey, *Int. J. Earth Sci.*, doi:10.1007/s00531-014-1092-8.
Çevikbaş, A., and Ö. Öztunalı (1991), Ore deposits in the Ulukışla-Çamardı (Niğde) Basin, *Jeol. Mühendisliği Derg.*, *39*, 22–40.
Cifelli, F., M. Mattei, M. Chadima, A. M. Hirt, and A. Hansen (2005), The origin of tectonic lineation in extensional basins: Combined neutron texture and magnetic analyses on "undeformed" clays, *Earth Planet. Sci. Lett.*, *235*(1), 62–78.
Čížková, H., and C. R. Bina (2015), Geodynamics of trench advance: Insights from a Philippine-Sea-style geometry, *Earth Planet. Sci. Lett.*, *430*, 408–415, doi:10.1016/j.epsl.2015.07.004.
Clark, M., and A. Robertson (2002), The role of the Early Tertiary Ulukisla Basin, southern Turkey, in suturing of the Mesozoic Tethys ocean, *J. Geol. Soc. Lond.*, *159*, 673–690, doi:10.1144/0016-764902-015.
Clark, M., and A. Robertson (2005), Uppermost Cretaceous-Lower Tertiary Ulukisla Basin, south-central Turkey: Sedimentary evolution of part of a unified basin complex within an evolving Neotethyan suture zone, *Sediment. Geol.*, *173*(1–4), 15–51, doi:10.1016/j.sedgeo.2003.12.010.
Clift, P., and P. Vannucchi (2004), Controls on tectonic accretion versus erosion in subduction zones: Implications for the origin and recycling of the continental crust, *Rev. Geophys.*, *42*, RG2001, doi:10.1029/2003RG000127.
Condon, D. J., B. Schoene, N. M. McLean, S. A. Bowring, and R. R. Parrish (2015), Metrology and traceability of U–Pb isotope dilution geochronology (EARTHTIME Tracer Calibration Part I), *Geochim. Cosmochim. Acta*, *164*, 464–480.
Corfu, F. (2004), U–Pb age, setting and tectonic significance of the anorthosite–mangerite–charnockite–granite suite, Lofoten–Vesterålen, Norway, *J. Petrol.*, *45*(9), 1799–1819.
Cox, A., and R. B. Hart (1986), *Plate Tectonics: How It Works*, 392 pp., Wiley-Blackwell, Malden, Mass.
Delibaş, O., and Y. Genc (2012), Late Cretaceous coeval acidic and basic magmatism, Karacaali magmatic complex, central Anatolia, Turkey, *Int. Geol. Rev.*, *54*(14), 1697–1720.
Demirtasli, E., N. Turhan, A. Z. Bilgin, and M. Selim (1984), Geology of the Bolkar mountains, in *Geology of the Taurus Belt. Proceedings of the International Symposium on the Geology of the Taurus Belt, Ankara, Turkey*, pp. 12–141, Mineral Resources and Exploration Institute of Turkey, Ankara.
Demirtaşlı, E., A. Z. Bilgin, F. Erenler, S. Işıklar, D. Sanlı, M. Selim, and N. Turhan (1973), Bolkardağlarının Jeolojisi, *Cumhuriyetin*, *50*, 42–67.
Dewey, J. F. (1980), Episodicity, sequence and style at convergent plate boundaries, in *The Continental Crust and its Mineral Deposits*, *Geol. Assoc. Can. Spec. Pap.*, vol. 20, edited by D. W. Strangway, 804 pp.
Dewey, J. F., and A. M. C. Şengör (1979), Aegean and surrounding regions: Complex multiplate and continuum tectonics in a convergent zone, *Bull. Geol. Soc. Am.*, *90*(1), 84–92, doi:10.1130/0016-7606(1979)90<84:AASRCM>2.0.CO;2.
Dilek, Y., P. Thy, B. Hacker, and S. Grundvig (1999), Structure and petrology of Tauride ophiolites and mafic dike intrusions (Turkey): Implications for the Neotethyan ocean, *Geol. Soc. Am. Bull.*, *111*(8), 1192–1216, doi:10.1130/0016-7606(1999)111<1192:SAPOTO>2.3.CO;2.
Dirik, R., M. C. Göncüoglu, and N. Kozlu (1999), Stratigraphy and pre-Miocene tectonic evolution of the southwestern part of the Sivas Basin, Central Anatolia, Turkey, *Geol. J.*, *34*, 303–319.
Dixon, J. E., and A. H. F. Robertson (Eds.) (1984), *The Geological Evolution of the Eastern Mediterranean*, Geological Society, London.
Doubrovine, P. V., B. Steinberger, and T. H. Torsvik (2012), Absolute plate motions in a reference frame defined by moving hot spots in the Pacific, Atlantic, and Indian oceans, *J. Geophys. Res.*, *117*, B09101, doi:10.1029/2011JB009072.
Espurt, N., J.-C. Hippolyte, N. Kaymakci, and E. Sangu (2014), Lithospheric structural control on inversion of the southern margin of the Black Sea Basin, Central Pontides, Turkey, *Lithosphere*, *6*(1), 26–34, doi:10.1130/l316.1.
Faccenna, C., et al. (2014), Mantle dynamics in the Mediterranean, *Rev. Geophys.*, *52*, 283–332, doi:10.1002/2013RG000444.
Fayon, A. K., D. L. Whitney, C. Teyssier, J. I. Garver, and Y. Dilek (2001), Effects of plate convergence obliquity on timing and mechanisms of exhumation of a mid-crustal terrain, the Central Anatolian Crystalline Complex, *Earth Planet. Sci. Lett.*, *192*, 191–205.
Fernández-Blanco, D., G. Bertotti, and A. Çiner (2013), Cenozoic tectonics of the Tuz Gölü Basin (Central Anatolian Plateau, Turkey), *Turkish J. Earth Sci.*, *715–738*, doi:10.3906/yer-1206-7.
Fuller, C. W., S. D. Willett, and M. T. Brandon (2006), Formation of forearc basins and their influence on subduction zone earthquakes, *Geology*, *34*(2), 65–68.
Funiciello, F., C. Faccenna, A. Heuret, S. Lallemand, E. Di Giuseppe, and T. W. Becker (2008), Trench migration, net rotation and slab-mantle coupling, *Earth Planet. Sci. Lett.*, *271*(1–4), 233–240, doi:10.1016/j.epsl.2008.04.006.
Gaina, C., and D. Müller (2007), Cenozoic tectonic and depth/age evolution of the Indonesian gateway and associated back-arc basins, *Earth Sci. Rev.*, *83*(3–4), 177–203, doi:10.1016/j.earscirev.2007.04.004.

Gautier, P., E. Bozkurt, E. Hallot, and K. Dirik (2002), Dating the exhumation of a metamorphic dome: Geological evidence for pre-Eocene unroofing of the Nigde Massif (Central Anatolia, Turkey), *Geol. Mag.*, *139*(05), 559–576, doi:10.1017/S0016756802006751.
Gautier, P., E. Bozkurt, V. Bosse, E. Hallot, and K. Dirik (2008), Coeval extensional shearing and lateral underflow during Late Cretaceous core complex development in the Niğde Massif, Central Anatolia, Turkey, *Tectonics*, *27*, TC1003, doi:10.1029/2006TC002089.
Göncüoğlu, M. C. (1986), Geochronological data from the southern part (Niğde area) of the Central Anatolian Massif, *Bull. Miner. Res. Explor. Inst. Turkey*, *105–106*(1978), 83–96.
Göncüoglu, M. C. (1997), Distribution of Lower Paleozoic rocks in the Alpine terranes of Turkey, *Early Paleoz. NW Gondwana*, *3*, 13–23.
Göncüoglu, M. C., V. Toprak, I. Kuscu, A. Erler, and E. Olgun (1991), Geology of the western part of the Central Anatolian Massif, *Part I South. Sect. Türkiye Pet. Anon. Ortakligi Rep.* (2909).
Göncüoglu, M. C., A. Erler, V. Toprak, K. M. Yaliniz, E. Olgun, and B. Rojay (1992), Orta Anadolu Masifinin orta bölümünün jeolojisi—bölüm 2: Orta kesim, *Turkish Pet. Corp. Rep.* (3155).
Görür, N., F. Y. Oktay, I. Seymen, and A. M. C. Sengor (1984), Palaeotectonic evolution of the Tuzgolu basin complex, Central Turkey: Sedimentary record of a Neo-Tethyan closure, *Geol. Soc. Lond. Spec. Publ.*, *17*(1), 467–482, doi:10.1144/GSL.SP.1984.017.01.34.
Görür, N., O. Tüysüz, and A. M. C. Şengör (1998), Tectonic evolution of the central Anatolian basins, *Int. Geol. Rev.*, *40*(9), 831–850.
Gülyüz, E., N. Kaymakci, M. J. M. Meijers, D. J. J. van Hinsbergen, C. Lefebvre, R. L. M. Vissers, B. W. H. Hendriks, and A. A. Peynircioglu (2013), Tectonophysics Late Eocene evolution of the Çiçekdağı Basin (central Turkey): Syn-sedimentary compression during microcontinent–continent collision in central Anatolia, *Tectonophysics*, *602*, 286–299, doi:10.1016/j.tecto.2012.07.003.
Gürer, D., D. van Hinsbergen, L. Matenco, N. Kaymakci, and F. Corfu (2014), Late Cretaceous to recent tectonic evolution of the Ulukisla Basin (Southern Central Anatolia), in *EGU General Assembly Conference Abstracts*, vol. 16, p. 12854.
Gürer, Ö. F., and E. Aldanmaz (2002), Origin of the Upper Cretaceous–Tertiary sedimentary basins within the Tauride–Anatolide platform in Turkey, *Geol. Mag.*, *139*(02), 191–197.
Gutnic, M., O. Monod, A. Poisson, and J.-F. Dumont (1979), Géologie des Taurides occidentales (Turquie), *Mém. Soc. Géol. Fr.*, *137*, 1–112.
Hall, R. (2002), Cenozoic geological and plate tectonic evolution of SE Asia and the SW Pacific: Computer-based reconstructions, model and animations, *J. Asian Earth Sci.*, *20*(4), 353–431, doi:10.1016/S1367-9120(01)00069-4.
Higgins, M., L. M. Schoenbohm, G. Brocard, N. Kaymakci, J. C. Gosse, and M. A. Cosca (2015), New kinematic and geochronologic evidence for the Quaternary evolution of the Central Anatolian fault zone (CAFZ), *Tectonics*, *34*, 2118–2141, doi:10.1002/2015TC003864.
Hrouda, F. (1982), Magnetic anisotropy of rocks and its application in geology and geophysics, *Geophys. Surv.*, *5*(1), 37–82.
Idleman, L., M. A. Cosca, M. T. Heizler, S. N. Thomson, C. Teyssier, and D. L. Whitney (2014), Tectonic burial and exhumation cycles tracked by muscovite and K-feldspar 40Ar/39Ar thermochronology in a strike-slip fault zone, central Turkey, *Tectonophysics*, *612–613*, 134–146, doi:10.1016/j.tecto.2013.12.003.
Ilbeyli, N. (2005), Mineralogical–geochemical constraints on intrusives in central Anatolia, Turkey: Tectono-magmatic evolution and characteristics of mantle source, *Geol. Mag.*, *142*(02), 187–207.
Ilbeyli, N., J. A. Pearce, M. F. Thirlwall, and J. G. Mitchell (2004), Petrogenesis of collision-related plutonics in Central Anatolia, Turkey, *Lithos*, *72*(3), 163–182.
Ilbeyli, N., J. A. Pearce, I. G. Meighan, and A. E. Fallick (2009), Contemporaneous Late Cretaceous calc-alkaline and alkaline magmatism in Central Anatolia, Turkey: O isotope constraints on petrogenesis, *Turkish J. Earth Sci.*, *18*(4), 529–547.
Innocenti, F., R. Mazzuoli, G. Pasquare, F. R. Di Brozolo, and L. Villari (1975), The Neogene calcalkaline volcanism of Central Anatolia: Geochronological data on Kayseri-Nigde area, *Geol. Mag.*, *112*(04), 349–360.
Isik, V. (2009), The ductile shear zone in granitoid of the Central Anatolian Crystalline Complex, Turkey: Implications for the origins of the Tuzgölü basin during the Late Cretaceous extensional deformation, *J. Asian Earth Sci.*, *34*(4), 507–521, doi:10.1016/j.jseaes.2008.08.005.
Isik, V., C.-H. Lo, C. Göncüoğlu, and S. Demirel (2008), 39 Ar/40 Ar ages from the Yozgat Batholith: Preliminary Data on the timing of Late Cretaceous extension in the Central Anatolian Crystalline Complex, Turkey, *J. Geol.*, *116*(5), 510–526, doi:10.1086/590922.
Jackson, M. (1991), Anisotropy of magnetic remanence: A brief review of mineralogical sources, physical origins, and geological applications, and comparison with susceptibility anisotropy, *Pure Appl. Geophys.*, *136*(1), 1–28.
Jackson, M., and L. Tauxe (1991), Anisotropy of magnetic susceptibility and remanence: Developments in the characterization of tectonic, sedimentary and igneous fabric, *Rev. Geophys.*, *29*, 371–376.
Jaffey, A. H., K. F. Flynn, L. E. Glendenin, W. C. T. Bentley, and A. M. Essling (1971), Precision measurement of half-lives and specific activities of U 235 and U 238, *Phys. Rev. C*, *4*(5), 1889.
Jaffey, N., and A. H. F. Robertson (2001), New sedimentological and structural data from the Ecemis Fault Zone, southern Turkey: Implications for its timing and offset and the Cenozoic tectonic escape of Anatolia, *J. Geol. Soc. Lond.*, *158*, 367–378, doi:10.1144/jgs.158.2.367.
Jaffey, N., and A. Robertson (2005), Non-marine sedimentation associated with Oligocene-Recent exhumation and uplift of the Central Taurus Mountains, S Turkey, *Sediment. Geol.*, *173*(1–4), 53–89, doi:10.1016/j.sedgeo.2003.11.025.
Jagoutz, O., L. Royden, A. F. Holt, and T. W. Becker (2015), Anomalously fast convergence of India and Eurasia caused by double subduction, *Nat. Geosci.*, *8*(6), 475–478, doi:10.1038/ngeo2418.
Jelinek, V. (1977), The statistical theory of measuring anisotropy of magnetic susceptibility of rocks and its application, *Geofyzika, Brno*, *87*(3), 4.
Jelínek, V., and R. V. Kropáček (1978), Statistical processing of anisotropy of magnetic susceptibility measured on groups of specimens, *Stud. Geophys. Geod.*, *22*(1), 50–62.
Jolivet, L., and J.-P. Brun (2010), Cenozoic geodynamic evolution of the Aegean, *Int. J. Earth Sci.*, *99*(1), 109–138.
Jolivet, L., et al. (2013), Aegean tectonics: Strain localisation, slab tearing and trench retreat, *Tectonophysics*, *597–598*, 1–33, doi:10.1016/j.tecto.2012.06.011.
Kadioglu, Y. K., Y. Dilek, N. Güleç, and K. A. Foland (2003), Tectonomagmatic evolution of bimodal plutons in the Central Anatolian Crystalline Complex, Turkey: A reply, *J. Geol.*, *111*(6), 671–690, doi:10.1086/430246.
Kadioglu, Y. K., Y. Dilek, and K. A. Foland (2006), Slab break-off and syncollisional origin of the Late Cretaceous magmatism in the Central Anatolian crystalline complex, Turkey, *Geol. Soc. Am. Spec. Pap.*, *409*(19), 381–415, doi:10.1130/2006.2409(19).
Karaoglan, F. (2016), Tracking the uplift of the Bolkar Mountains (south-central Turkey): Evidence from apatite fission track thermochronology, *Turkish J. Earth Sci.*, *25*, 64–80, doi:10.3906/yer-1504-17.
Kaymakci, N., C. E. Duermeijer, C. Langereis, S. H. White, and P. M. Van Dijk (2003), Palaeomagnetic evolution of the Çankırı Basin (central Anatolia, Turkey): Implications for oroclinal bending due to indentation, *Geol. Mag.*, *140*(3), 343–355, doi:10.1017/S001675680300757X.
Kaymakci, N., Y. Özçelik, S. H. White, and P. M. Van Dijk (2009), Tectono-stratigraphy of the Çankırı Basin: Late Cretaceous to early Miocene evolution of the Neotethyan Suture Zone in Turkey, *Geol. Soc. Lond. Spec. Publ.*, *311*(1), 67–106, doi:10.1144/sp311.3.
Kergaravat, C., C. Ribes, E. Legeay, J.-P. Callot, K. S. Kavak, and J.-C. Ringenbach (2016), Minibasins and salt canopy in foreland fold-and-thrust belts: The central Sivas Basin, Turkey, *Tectonics*, *35*, 1342–1366, doi:10.1002/2016TC004186.

Keskin, M. (2007), Eastern Anatolia: A hotspot in a collision zone without a mantle plume, *Geol. Soc. Am. Spec. Pap.*, *2430*(32), doi:10.1130/2007.2430(32).
Ketin, I., and I. Akarsu (1965), Ulukisla Tersiyer Havzasinin Jeolojik Etüdü Hakkinda Rapor, *TPAO Rap.*, *339*, 12–20.
Koç, A., N. Kaymakci, D. J. J. van Hinsbergen, and R. L. M. Vissers (2014), A Miocene onset of the modern extensional regime in the Isparta Angle: Constraints from the Yalvaç Basin (southwest Turkey), *Int. J. Earth Sci.*, *1963*, doi:10.1007/s00531-014-1100-z.
Koç, A., D. J. J. van Hinsbergen, N. Kaymakci, and C. G. Langereis (2015), Late Neogene oroclinal bending in the central Taurides: A record of terminal eastward subduction in southern Turkey?, *Earth Planet. Sci. Lett.*, *1*, doi:10.1016/j.epsl.2015.11.020.
Kocak, K., and B. E. Leake (1994), The petrology of the Ortakoy district and its ophiolite at the western edge of the Middle Anatolian Massif, Turkey, *J. Afr. Earth Sci.*, *18*(2), 163–174.
Koçyigit, A. (1991), An example of an accretionary forearc basin from northern Central Anatolia and its implications for the history of subduction of Neo-Tethys in Turkey, *Geol. Soc. Am. Bull.*, *103*(1), 22–36, doi:10.1130/0016-7606(1991)103<0022:AEOAAF>2.3.CO;2.
Koçyiğit, A., and A. Beyhan (1998), A new intracontinental transcurrent structure: The Central Anatolian Fault Zone, Turkey, *Tectonophysics*, *284*(3), 317–336.
Köksal, S., and M. C. Göncüoglu (1997), Geology of the Idis Dagi-Avanos Area (Nevsehir-Central Anatolia), *Miner. Res. Expl. Bull.*, *119*, 41–58.
Köksal, S., A. Möller, M. C. Göncüoglu, D. Frei, and A. Gerdes (2012), Crustal homogenization revealed by U–Pb zircon ages and Hf isotope evidence from the Late Cretaceous granitoids of the Agaçören intrusive suite (Central Anatolia/Turkey), *Contrib. Mineral. Petrol.*, *163*(4), 725–743, doi:10.1007/s00410-011-0696-2.
Köksal, S., F. Toksoy-Köksal, M. C. Göncüoglu, A. Möller, A. Gerdes, and D. Frei (2013), Crustal source of the Late Cretaceous Satansari monzonite stock (central Anatolia–Turkey) and its significance for the Alpine geodynamic evolution, *J. Geodyn.*, *65*, 82–93.
Krogh, T. E. (1973), A low-contamination method for hydrothermal decomposition of zircon and extraction of U and Pb for isotopic age determinations, *Geochim. Cosmochim. Acta*, *37*(3), 485–494.
Kurt, M. A., M. Alpaslan, M. C. Göncüoğlu, and A. Temel (2008), Geochemistry of late stage medium to high-K calc-alkaline and shoshonitic dykes in the Ulukişla Basin (Central Anatolia, Turkey): Petrogenesis and tectonic setting, *Geochem. Int.*, *46*(11), 1145–1163.
Lefebvre, C., A. Barnhoorn, D. J. J. van Hinsbergen, N. Kaymakci, and R. L. M. Vissers (2011), Late Cretaceous extensional denudation along a marble detachment fault zone in the Kırşehir massif near Kaman, central Turkey, *J. Struct. Geol.*, *33*(8), 1220–1236, doi:10.1016/j.jsg.2011.06.002.
Lefebvre, C., M. J. M. Meijers, N. Kaymakci, A. Peynircioğlu, C. G. Langereis, and D. J. J. van Hinsbergen (2013), Reconstructing the geometry of central Anatolia during the late Cretaceous: Large-scale Cenozoic rotations and deformation between the Pontides and Taurides, *Earth Planet. Sci. Lett.*, *366*, 83–98, doi:10.1016/j.epsl.2013.01.003.
Lefebvre, C., M. Kalijn Peters, P. C. Wehrens, F. M. Brouwer, and H. L. M. van Roermund (2015), Thermal history and extensional exhumation of a high-temperature crystalline complex (Hırkadağ Massif, Central Anatolia), *Lithos*, *238*, 156–173, doi:10.1016/j.lithos.2015.09.021.
Lepetit, P., et al. (2014), 40 Ar/39 Ar dating of ignimbrites and plinian air-fall layers from Cappadocia, Central Turkey: Implications to chronostratigraphic and Eastern Mediterranean palaeoenvironmental record, *Chemie der Erde-Geochem.*, *74*(3), 471–488.
Ludwig, K. R. (2009), Isoplot 4.1. A geochronological toolkit for Microsoft Excel, *Berkeley Geochronol. Cent. Spec. Publ.*, *4*, 76.
Maffione, M., S. Pucci, L. Sagnotti, and F. Speranza (2012), Magnetic fabric of Pleistocene continental clays from the hanging-wall of an active low-angle normal fault (Altotiberina Fault, Italy), *Int. J. Earth Sci.*, *101*(3), 849–861.
Maffione, M., C. Hernandez-Moreno, M. C. Ghiglione, F. Speranza, D. J. J. van Hinsbergen, and E. Lodolo (2015), Constraints on deformation of the Southern Andes since the Cretaceous from anisotropy of magnetic susceptibility, *Tectonophysics*, *665*, 236–250.
Mattei, M., L. Sagnotti, C. Faccenna, and R. Funiciello (1997), Magnetic fabric of weakly deformed clay-rich sediments in the Italian peninsula: Relationship with compressional and extensional tectonics, *Tectonophysics*, *271*(1), 107–122.
Mattinson, J. M. (2005), Zircon U–Pb chemical abrasion ("CA-TIMS") method: Combined annealing and multi-step partial dissolution analysis for improved precision and accuracy of zircon ages, *Chem. Geol.*, *220*(1), 47–66.
Mattinson, J. M. (2010), Analysis of the relative decay constants of 235 U and 238 U by multi-step CA-TIMS measurements of closed-system natural zircon samples, *Chem. Geol.*, *275*(3), 186–198.
McLean, N. M., D. J. Condon, B. Schoene, and S. A. Bowring (2015), Evaluating uncertainties in the calibration of isotopic reference materials and multi-element isotopic tracers (EARTHTIME Tracer Calibration Part II), *Geochim. Cosmochim. Acta*, *164*, 481–501.
Meijers, M. J. M., N. Kaymakci, D. J. J. van Hinsbergen, C. G. Langereis, R. A. Stephenson, and J. C. Hippolyte (2010), Late Cretaceous to Paleocene oroclinal bending in the central Pontides (Turkey), *Tectonics*, *29*, TC4016, doi:10.1029/2009TC002620.
Meijers, M. J. M., B. E. Strauss, M. Özkaptan, J. M. Feinberg, A. Mulch, D. L. Whitney, and N. Kaymakçi (2016), Age and paleoenvironmental reconstruction of partially remagnetized lacustrine sedimentary rocks (Oligocene Aktoprak basin, central Anatolia, Turkey), *Geochem. Geophys. Geosyst.*, *17*, 914–939, doi:10.1002/2015GC006209.
Menant, A., L. Jolivet, and B. Vrielynck (2016), Kinematic reconstructions and magmatic evolution illuminating crustal and mantle dynamics of the eastern Mediterranean region since the late Cretaceous, *Tectonophysics*, *675*, 103–140.
Monod, O. (1977), Recherches géologiques dans le Taurus occidental au Sud de Beysehir (Turquie), Univ. Paris Sud, Orsay, France.
Nairn, S. P., A. H. F. Robertson, U. C. Unlugenc, K. Tasli, and N. Inan (2012), Tectonostratigraphic evolution of the Upper Cretaceous-Cenozoic central Anatolian basins: An integrated study of diachronous ocean basin closure and continental collision, *Geol. Soc. Lond. Spec. Publ.*, *372*(1), 343–384, doi:10.1144/SP372.9.
Nikishin, A. M., A. I. Okay, O. Tüysüz, A. Demirer, N. Amelin, and E. Petrov (2015), The Black Sea basins structure and history: New model based on new deep penetration regional seismic data. Part 1: Basins structure and fill, *Mar. Pet. Geol.*, *59*, 638–655, doi:10.1016/j.marpetgeo.2014.08.017.
Okay, A. I. (1986), High-pressure/low-temperature rocks of Turkey, in *Blueschists and Eclogites*, *Geol. Soc. Am. Mem.*, edited by B. W. Evans and E. H. Brown, pp. 333–347.
Okay, A. I., and A. M. Nikishin (2015), Tectonic evolution of the southern margin of Laurasia in the Black Sea region, *Int. Geol. Rev.*, 1–26, doi:10.1080/00206814.2015.1010609.
Okay, A. I., and O. Tüysüz (1999), Tethyan sutures of northern Turkey, *Geol. Soc. Lond. Spec. Publ.*, *156*(1), 475–515, doi:10.1144/GSL.SP.1999.156.01.22.
Okay, A. I., M. Satir, H. Maluski, M. Sikayo, P. Monié, R. Metzger, and S. Akyüz (1996), Paleo- and Neo-Tethyan events in northwestern Turkey: Geologic and geochronologic constraints, in *The Tectonic Evolution of Asia*, edited by A. Yin and T. M. Harisson, pp. 420–441, Cambridge Univ. Press, Cambridge.
Okay, A. I., I. Tansel, and O. Tüysüz (2001), Obduction, subduction and collision as reflected in the Upper Cretaceous–Lower Eocene sedimentary record of western Turkey, *Geol. Mag.*, *138*(02), 117–142, doi:10.1017/S0016756801005088.

Okay, A. I., O. Tüysüz, M. Satır, S. Özkan-Altıner, D. Altıner, S. Sherlock, and R. H. Eren (2006), Cretaceous and Triassic subduction-accretion, high-pressure-low-temperature metamorphism, and continental growth in the Central Pontides, Turkey, *Geol. Soc. Am. Bull.*, *118*(9–10), 1247–1269, doi:10.1130/B25938.1.

Oktay, F. Y. (1973), Sedimentary and tectonic history of the Ulukisla area, southern Turkey, University of London.

Oktay, F. Y. (1981), Stratigraphy and geological evolution of the sedimentary cover of the central Anatolian Massif in the Kaman-Kirs ehir region. Turkish Geological Society, 35th Scientific and Technical Assembly, in *Symposium on the Geology of central Anatolia*.

Oktay, F. Y. (1982), Stratigraphy and geological history of Ulukısla and its surroundings, *Bull. Turkish Geol. Soc.*, *25*, 15–23.

Önen, P., and R. Hall (2000), Sub-ophiolite metamorphic rocks from NW Anatolia, Turkey, *J. Metamorph. Geol.*, *18*(5), 483–495, doi:10.1046/j.1525-1314.2000.00276.x.

Özdamar, Ş., M. Z. Billor, G. Sunal, F. Esenli, and M. F. Roden (2013), First U-Pb SHRIMP zircon and 40Ar/39Ar ages of metarhyolites from the Afyon-Bolkardag Zone, SW Turkey: Implications for the rifting and closure of the Neo-Tethys, *Gondwana Res.*, *24*(1), 377–391, doi:10.1016/j.gr.2012.10.006.

Özgül, N. (1984), Stratigraphy and tectonic evolution of the Central Taurides, *Geol. Taurus Belt*, 77–90.

Özsayin, E., T. A. Ciner, F. B. Rojay, R. K. Dirik, D. Melnick, and D. Fernandez-Blanco (2013), Plio-Quaternary extensional tectonics of the Central Anatolian Plateau: A case study from the Tuz Gölü Basin, Turkey, *Turkish J. Earth Sci.*, *22*(5), 691–714.

Parés, J. M. (2004), How deformed are weakly deformed mudrocks? Insights from magnetic anisotropy, *Geol. Soc. Lond. Spec. Publ.*, *238*(1), 191–203.

Parés, J. M., and B. A. van der Pluijm (2002), Evaluating magnetic lineations (AMS) in deformed rocks, *Tectonophysics*, *350*(4), 283–298.

Parlak, O., and M. Delaloye (1999), Precise 40Ar/39Ar ages from the metamorphic sole of the Mersin ophiolite (southern Turkey), *Tectonophysics*, *301*, 145–158.

Parlak, O., V. Hock, and M. Delaloye (2000), Suprasubduction zone origin of the Pozanti-Karsanti Ophiolite (Southern Turkey) Deduced from Whole-rock and Mineral Chemistry of the Gabbroic Cumulates, *Geol. Soc. Lond. Spec. Publ.*, *173*(1), 219–234, doi:10.1144/GSL.SP.2000.173.01.11.

Parlak, O., F. Karaoğlan, T. Rizaoğlu, U. Klötzli, F. Koller, and Z. Billor (2013), U-Pb and 40Ar-39Ar geochronology of the ophiolites and granitoids from the Tauride belt: Implications for the evolution of the Inner Tauride suture, *J. Geodyn.*, *65*, 22–37, doi:10.1016/j.jog.2012.06.012.

Pichat, A., G. Hoareau, J.-P. Callot, and J.-C. Ringenbach (2016), Diagenesis of Oligocene continental sandstones in salt-walled mini-basins—Sivas Basin, Turkey, *Sediment. Geol.*, *339*, 13–31.

Poisson, A., J. C. Guezou, A. Ozturk, S. Inan, H. Temiz, H. Gürsöy, K. S. Kavak, and S. Özden (1996), Tectonic setting and evolution of the Sivas Basin, Central Anatolia, Turkey, *Int. Geol. Rev.*, *38*(9), 838–853, doi:10.1080/00206819709465366.

Poisson, A., et al. (2016), Miocene transgression in the central and eastern parts of the Sivas Basin (Central Anatolia, Turkey) and the Cenozoic palaeogeographical evolution, *Int. J. Earth Sci.*, *105*(1), 339–368, doi:10.1007/s00531-015-1248-1.

Pourteau, A., O. Candan, and R. Oberhänsli (2010), High-pressure metasediments in central Turkey: Constraints on the Neotethyan closure history, *Tectonics*, *29*, TC5004, doi:10.1029/2009TC002650.

Pourteau, A., M. Sudo, O. Candan, P. Lanari, O. Vidal, and R. Oberhänsli (2013), Neotethys closure history of Anatolia: Insights from 40 Ar- 39 Ar geochronology and P-T estimation in high-pressure metasedimentary rocks, *J. Metamorph. Geol.*, *31*, 585–606, doi:10.1111/jmg.12034.

Pourteau, A., R. Bousquet, O. Vidal, A. Plunder, E. Duesterhoeft, O. Candan, and R. Oberhänsli (2014), Multistage growth of Fe–Mg–carpholite and Fe–Mg–chloritoid, from field evidence to thermodynamic modelling, *Contrib. Mineral. Petrol.*, *168*(6), 1090, doi:10.1007/s00410-014-1090-7.

Radeff, G., D. Cosentino, T. Schildgen, M. R. Strecker, P. Cipollari, G. Darbas, and K. Gürbüz (2012), Uplift of the SE Margin of the Central Anatolian Plateau: Temporal constraints from the Adana Basin, Southern Turkey, in *AGU Fall Meeting Abstracts*, vol. 1, p. 6.

Reilinger, R., S. McClusky, D. Paradissis, S. Ergintav, and P. Vernant (2010), Geodetic constraints on the tectonic evolution of the Aegean region and strain accumulation along the Hellenic subduction zone, *Tectonophysics*, *488*(1–4), 22–30, doi:10.1016/j.tecto.2009.05.027.

Ribes, C., C. Kergaravat, C. Bonnel, P. Crumeyrolle, J.-P. Callot, A. Poisson, H. Temiz, and J.-C. Ringenbach (2015), Fluvial sedimentation in a salt-controlled mini-basin: Stratal patterns and facies assemblages, Sivas Basin, Turkey, *Sedimentology*, *62*(6), 1513–1545.

Rimmelé, G., T. Parra, B. Goffé, R. Oberhänsli, L. Jolivet, and O. Cadan (2005), Exhumation paths of high-pressure-low-temperature metamorphic rocks from the Lycian Nappes and the Menderes Massif (SW Turkey): A multi-equilibrium approach, *J. Petrol.*, *46*(3), 641–669, doi:10.1093/petrology/egh092.

Robertson, A. H. F. (2000), Mesozoic-Tertiary tectonic-sedimentary evolution of a south Tethyan Oceanic Basin and its margins in Southern Turkey, *Geol. Soc. Lond. Spec. Publ.*, *173*(1), 97–138, doi:10.1144/GSL.SP.2000.173.01.05.

Robertson, A. H. F., and J. E. Dixon (1984), Introduction: Aspects of the geological evolution of the Eastern Mediterranean, *Geol. Soc. Lond. Spec. Publ.*, *17*(1), 1–74, doi:10.1144/GSL.SP.1984.017.01.02.

Robertson, A. H. F., O. Parlak, and T. Ustaomer (2009), Melange genesis and ophiolite emplacement related to subduction of the northern margin of the Tauride-Anatolide continent, central and western Turkey, *Geol. Soc. Lond. Spec. Publ.*, *311*(1), 1, doi:10.1144/SP311.Erratum.

Robertson, A. H. F., O. Parlak, and T. Ustaömer (2012), Overview of the Palaeozoic–Neogene evolution of Neotethys in the Eastern Mediterranean region (southern Turkey, Cyprus, Syria), *Pet. Geosci.*, *18*(4), 381–404, doi:10.1144/petgeo2011-091.

Rochette, P., M. Jackson, and C. Aubourg (1992), Rock magnetism and the interpretation of anisotropy of magnetic susceptibility, *Rev. Geophys.*, *30*(3), 209–226, doi:10.1029/92RG00733.

Sagnotti, L., and F. Speranza (1993), Magnetic fabric analysis of the Plio-Pleistocene clayey units of the Sant'Arcangelo Basin, southern Italy, *Phys. Earth Planet. Inter.*, *77*(3–4), 165–176.

Sagnotti, L., F. Speranza, A. Winkler, M. Mattei, and R. Funiciello (1998), Magnetic fabric of clay sediments from the external northern Apennines (Italy), *Phys. Earth Planet. Inter.*, *105*(1), 73–93.

Sarıkaya, M. A., C. Yıldırım, and A. Çiner (2015), No surface breaking on the Ecemiş Fault, central Turkey, since Late Pleistocene (~64.5 ka): New geomorphic and geochronologic data from cosmogenic dating of offset alluvial fans, *Tectonophysics*, *649*, 33–46.

Schärer, U. (1984), The effect of initial 230 Th disequilibrium on young U Pb ages: The Makalu case, Himalaya, *Earth Planet. Sci. Lett.*, *67*(2), 191–204.

Schellart, W. P., D. R. Stegman, and J. Freeman (2008), Global trench migration velocities and slab migration induced upper mantle volume fluxes: Constraints to find an Earth reference frame based on minimizing viscous dissipation, *Earth Sci. Rev.*, *88*(1–2), 118–144, doi:10.1016/j.earscirev.2008.01.005.

Schildgen, T. F., D. Cosentino, A. Caruso, R. Buchwaldt, C. Yıldırım, S. A. Bowring, B. Rojay, H. Echtler, and M. R. Strecker (2012), Surface expression of eastern Mediterranean slab dynamics: Neogene topographic and structural evolution of the southwest margin of the Central Anatolian Plateau, Turkey, *Tectonics*, *31*, TC2005, doi:10.1029/2011TC003021.

Şengör, A. M. C., and Y. Yılmaz (1981), Tethyan evolution of Turkey: A plate tectonic approach, *Tectonophysics*, *75*, 181–241.

Seno, T., and S. Maruyama (1984), Paleogeographic reconstruction and origin of the Philippine Sea, *Tectonophysics*, *102*(1), 53–84.
Sosson, M., et al. (2015), The eastern Black Sea-Caucasus region during the Cretaceous: New evidence to constrain its tectonic evolution, *C. R. Geosci.*, *348*, 23–32, doi:10.1016/j.crte.2015.11.002.
Soto, R., J. C. Larrasoaña, L. E. Arlegui, E. Beamud, B. Oliva-Urcia, and J. L. Simón (2009), Reliability of magnetic fabric of weakly deformed mudrocks as a palaeostress indicator in compressive settings, *J. Struct. Geol.*, *31*(5), 512–522.
Stacey, J. S., and J. D. Kramers (1975), Approximation of terrestrial lead isotope evolution by a two-stage model, *Earth Planet. Sci. Lett.*, *26*(2), 207–221.
Stern, C. R. (2011), Subduction erosion: Rates, mechanisms, and its role in arc magmatism and the evolution of the continental crust and mantle, *Gondwana Res.*, *20*(2–3), 284–308, doi:10.1016/j.gr.2011.03.006.
Stern, R. J., M. K. Reagan, O. Ishizuka, Y. Ohara, and S. A. Whattam (2012), To understand subduction initiation, study forearc crust: To understand forearc crust, study ophiolites, *Lithosphere*, *4*, 469–483, doi:10.1130/L183.1.
Tarling, D., and F. Hrouda (1993), *Magnetic Anisotropy of Rocks*, 217 pp., Chapman and Hall, London.
Toprak, V., and M. C. Göncöoğlu (1993), Tectonic control on the development of the Neogene-Quaternary Central Anatolian Volcanic Province, Turkey, *Geol. J.*, *28*(3–4), 357–369.
Ulu, Ü. (2009), Turkish Geological Map Series, Karaman M33.
Umhoefer, P. J., D. L. Whitney, C. Teyssier, A. K. Fayon, G. Casale, T. Heizler, and M. T. Heizler (2007), Yo-yo tectonics in a wrench zone, Central Anatolian fault zone, Turkey, *Geol. Soc. Am. Spec. Pap.*, *434*(303), 35–57, doi:10.1130/2007.2434(03).
Ünadan, G., and V. Yüksel (1978), Eski Bir Graben Örnegi: Haymana-Polatli Havzasi, *TJK Bülteni, C*, *21*, 165–169.
Ustaömer, T., and A. H. F. Robertson (1997), Tectonic-sedimentary evolution of the North Tethyan Margin in the Central Pontides of Northern Turkey, *AAPG Mem.*, *68*, 255–290.
Ustaömer, T., and A. H. F. Robertson (2010), Late Palaeozoic-Early Cenozoic tectonic development of the Eastern Pontides (Artvin area), Turkey: Stages of closure of Tethys along the southern margin of Eurasia, *Geol. Soc. Lond. Spec. Publ.*, *340*(1), 281–327.
Uyeda, S., and H. Kanamori (1979), Back-arc opening and the mode of subduction, *J. Geophys. Res.*, *84*(B3), 1049–1061, doi:10.1029/JB084iB03p01049.
van Hinsbergen, D. J. J., and S. M. Schmid (2012), Map view restoration of Aegean–West Anatolian accretion and extension since the Eocene, *Tectonics*, *31*, TC5005, doi:10.1029/2012TC003132.
van Hinsbergen, D. J. J., et al. (2015), Dynamics of intraoceanic subduction initiation: 2. Suprasubduction zone ophiolite formation and metamorphic sole exhumation in context of absolute plate motions, *Geochem. Geophys. Geosyst.*, *16*, 1771–1785, doi:10.1002/2015GC005746.
van Hinsbergen, D. J. J., et al. (2016), Tectonic evolution and paleogeography of the Kırşehir Block and the Central Anatolian Ophiolites, *Tectonics*, *35*, 983–1014, doi:10.1002/2015TC004018.
van Hunen, J., and M. S. Miller (2015), Collisional processes and links to episodic changes in subduction zones, *Elements*, *11*(2), 119–124, doi:10.2113/gselements.11.2.119.
von Huene, R., and D. W. Scholl (1991), Observations at convergent margins concerning sediment subduction, subduction erosion, and the growth of continental crust, *Rev. Geophys.*, *29*(3), 279–316, doi:10.1029/91RG00969.
von Huene, R., C. R. Ranero, and P. Vannucchi (2004), Generic model of subduction erosion, *Geology*, *32*(10), 913–916, doi:10.1130/G20563.1.
Weil, A. B., and A. Yonkee (2009), Anisotropy of magnetic susceptibility in weakly deformed red beds from the Wyoming salient, Sevier thrust belt: Relations to layer-parallel shortening and orogenic curvature, *Lithosphere*, *1*(4), 235–256.
Whitney, D. L., and Y. Dilek (1997), Core complex development in central Anatolia, Turkey, *Geology*, doi:10.1130/0091-7613(1997)025<1023.
Whitney, D. L., and Y. Dilek (1998), Metamorphism during alpine crustal thickening and extension in central Anatolia, Turkey: The Nigde metamorphic core complex, *J. Petrol.*, *39*(7), 1385–1403.
Whitney, D. L., and M. A. Hamilton (2004), Timing of high-grade metamorphism in central Turkey and the assembly of Anatolia, *J. Geol. Soc. Lond.*, *161*, 823–828.
Whitney, D. L., C. Teyssier, Y. Dilek, and A. K. Fayon (2001), Metamorphism of the Central Anatolian Crystalline Complex, Turkey: Influence of orogen-normal collision vs. wrench-dominated tectonics on P–T–t paths, *J. Metamorph. Geol.*, *19*, 411–432.
Whitney, D. L., C. Teyssier, A. K. Fayon, M. A. Hamilton, and M. Heizler (2003), Tectonic controls on metamorphism, partial melting, and intrusion: Timing and duration of regional metamorphism and magmatism in the Niğde Massif, Turkey, *Tectonophysics*, *376*(1–2), 37–60, doi:10.1016/j.tecto.2003.08.009.
Whitney, D. L., C. Teyssier, and M. T. Heizler (2007), Gneiss domes, metamorphic core complexes, and wrench zones: Thermal and structural evolution of the Niğde Massif, central Anatolia, *Tectonics*, *26*, TC5002, doi:10.1029/2006TC002040.
Whitney, D. L., C. Teyssier, S. C. Kruckenberg, V. L. Morgan, and L. J. Iredale (2008), High-pressure–low-temperature metamorphism of metasedimentary rocks, southern Menderes Massif, western Turkey, *Lithos*, *101*(3–4), 218–232, doi:10.1016/j.lithos.2007.07.001.
Williams, S., N. Flament, R. Dietmar Müller, and N. Butterworth (2015), Absolute plate motions since 130 Ma constrained by subduction zone kinematics, *Earth Planet. Sci. Lett.*, *418*, 66–77, doi:10.1016/j.epsl.2015.02.026.
Wu, J., J. Suppe, R. Lu, and R. Kanda (2016), Philippine Sea and East Asian plate tectonics since 52 Ma constrained by new subducted slab reconstruction methods, *J. Geophys. Res. Solid Earth*, *121*, 4670–4741, doi:10.1002/2016JB012923.
Yaliniz, K. M., N. S. Aydin, M. C. Göncüoglu, and O. Parlak (1999), Terlemez quartz monzonite of Central Anatolia (Aksaray-Sarikaraman): Age, petrogenesis and geotectonic implications for ophiolite emplacement, *Geol. J.*, *34*(3), 233–242, doi:10.1002/(SICI)1099-1034(199907/09)34:3<233::AID-GJ824>3.0.CO;2-5.
Yaliniz, M. K. (2008), A geochemical attempt to distinguish forearc and back arc ophiolites from the "supra-subduction" central anatolian ophiolites (Turkey) by comparison with modern oceanic analogues, *Ofioliti*, *33*(2), 119–129, doi:10.4454/ofioliti.v33i2.363.
Yaliniz, M. K., and M. C. Göncüoglu (1998), General geological characteristics and distribution of the Central Anatolian Ophiolites, *Yerbilimleri*, *20*, 19–30.
Yaliniz, M. K., P. A. Floyd, and M. C. Goncuoglu (1996), Supra-subduction zone ophiolites of Central Anatolia: Geochemical evidence from the Sarikaraman Ophiolite, Aksaray, Turkey, *Mineral. Mag.*, *60*, 697–710.
Yaliniz, M. K., M. C. Göncüoglu, and S. Özkan-Altıner (2000a), Formation and emplacement ages of the SSZ-type Neotethyan ophiolites in Central Anatolia, Turkey: Palaeotectonic implications, *Geol. J.*, *35*, 42–57.
Yaliniz, M. K., P. A. Floyd, and M. C. Göncüoglu (2000b), Geochemistry of volcanic rocks from the Çiçekdag Ophiolite, Central Anatolia, Turkey, and their inferred tectonic setting within the northern branch of the Neotethyan Ocean, *Geol. Soc. Lond. Spec. Publ.*, *173*, 203–218.
Yetiş, C. (1968), Geology of the Çamardı (Niğde) region and the characteristics of the Ecemiş Fault Zone between Maden Boğazi and Kamışlıç, *Üniversitesi Fen Fak. Mecmuası, Seri B*, *43*(43), 41–61.
Yetis, C. (1984), New observations on the age of the Ecemis Fault, *Geol. Taurus Belt. Maden Tektik Aram. Enstitüsü, Ankara, Turkey Tekeli O Goncuoglu MC*, 159–164.

Yetiş, C., G. Kelling, S. L. Gökçen, and F. Baroz (1995), A revised stratigraphic framework for later Cenozoic sequences in the northeastern Mediterranean region, *Geol. Rundschau*, *84*(4), 794–812, doi:10.1007/BF00240569.

Yıldırım, C., M. A. Sarıkaya, and A. Çiner (2016), Late Pleistocene intraplate extension of the Central Anatolian Plateau, Turkey: Inferences from cosmogenic exposure dating of alluvial fan, landslide and moraine surfaces along the *Ecemiş Fault Zone. Tectonics*, *35*, doi:10.1002/2015TC004038.

Yılmaz, A., and H. Yılmaz (2006), Characteristic features and structural evolution of a post collisional basin: The Sivas Basin, Central Anatolia, Turkey, *J. Asian Earth Sci.*, *27*(2), 164–176.

Zahirovic, S., M. Seton, and R. D. Müller (2014), The Cretaceous and Cenozoic tectonic evolution of Southeast Asia, *Solid Earth*, *5*(1), 227–273, doi:10.5194/se-5-227-2014.